Thermoelectric Silicon: From Fundamental Physics to Real-World Applications

Dario Narducci
Dept. of Materials Science, Univ. of Milano Bicocca, Milano, Italy
dario.narducci@unimib.it

Outline

- Why Heat Harvesting Matters
- Thermoelectricity: Physics and Technology
- Materials Issues
- Silicon as a New Player for Thermoelectrics:
  - SiGe alloys for RTGs
  - Si at low temperatures: Nanowires
  - Si at low temperatures: Thin Films
- From Materials to Devices
- Applications
- Some Conclusions

Why Heat Harvesting Matters

Estimated U.S. Energy Consumption in 2021: 97.3 Quads

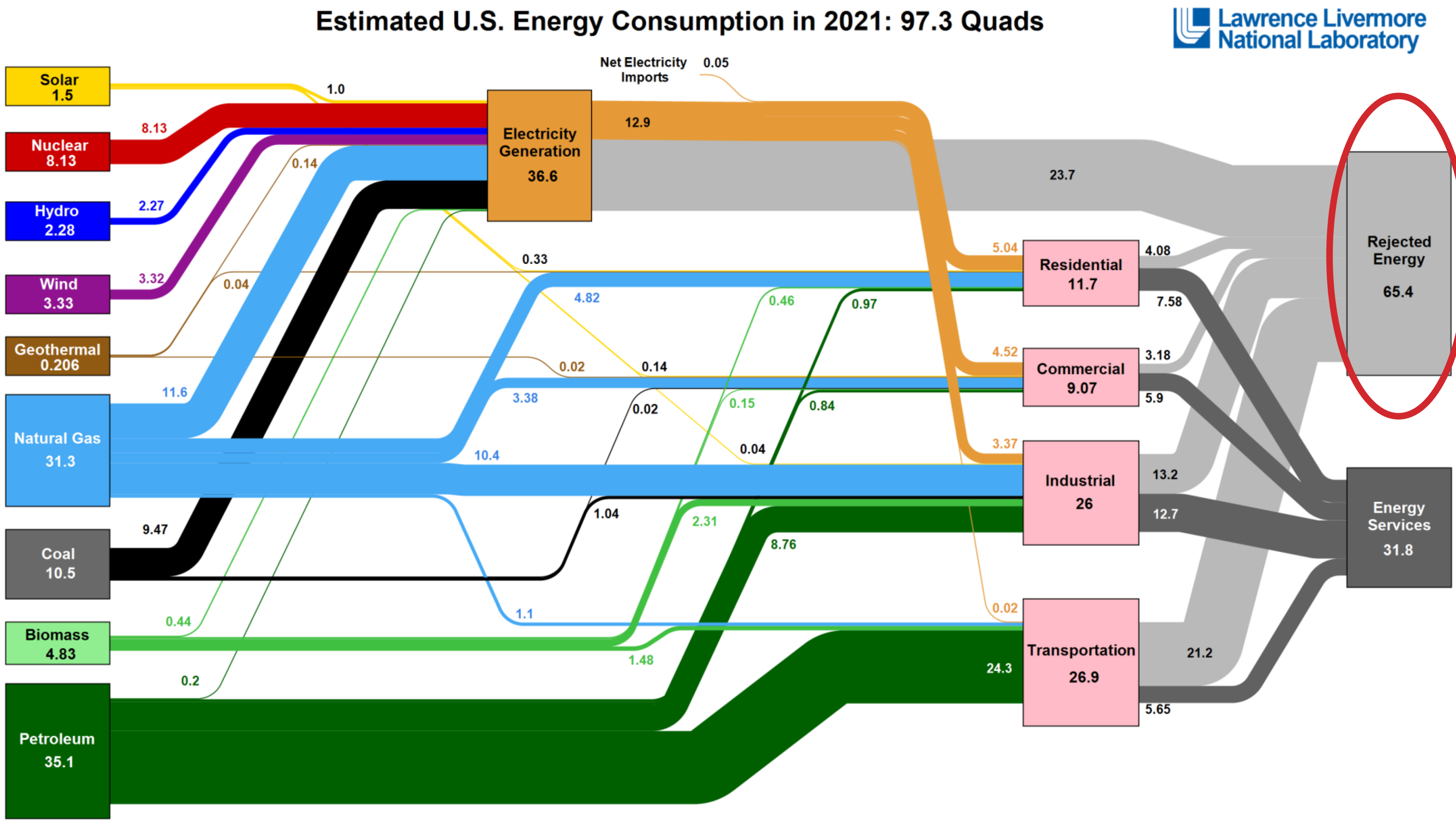

Source: LLNL March, 2022. Data is based on DOE/EIA MER (2021). If this information or a reproduction of it is used, credit must be given to the Lawrence Livermore National Laboratory and the Department of Energy, under whose auspices the work was performed. Distributed electricity represents only retail electricity sales and does not include self-generation. EIA reports consumption of renewable resources (i.e., hydro, wind, geothermal and solar) for electricity in BTU-equivalent values by assuming a typical fossil fuel plant heat rate. The efficiency of electricity production is calculated as the total retail electricity delivered divided by the primary energy input into electricity generation. End use efficiency is estimated as 65% for the residential sector, 65% for the commercial sector, 21% for the transportation sector and 49% for the industrial sector, which was updated in 2017 to reflect DOE's analysis of manufacturing. Totals may not equal sum of components due to independent rounding. LLNL-MI-410527

Why Heat Harvesting Matters

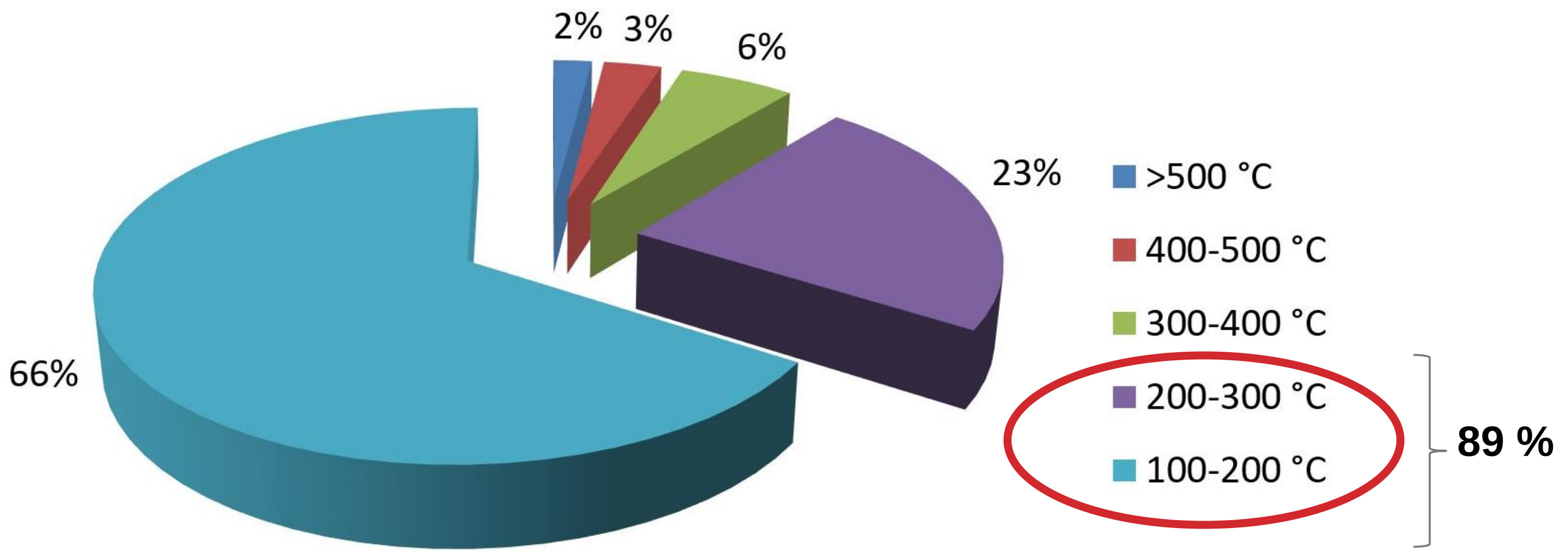

Thermoelectricy and Classical Irreversible Thermodynamics

$$\begin{cases} J_q = \kappa T^2 \dfrac{d(1/T)}{dx} \\ J_e = \qquad \sigma T \left(\dfrac{F}{T} \right) \end{cases}$$

Fourier's law

Ohm's law

In an open circuit ($J_e = 0$), $-L_{eq} \dfrac{dT}{dx} + \sigma F T^2 = 0$ so that

$$L_{eq} = \sigma T^2 \left(-\frac{\Delta V}{\Delta T} \right) = \sigma T^2 \alpha$$

In a short circuit and for $\dfrac{dT}{dx} = 0$ we get $J_q / J_e = L_{qe} / (\sigma T)$ whence

$$\Pi \equiv J_q / J_e = \sigma T^2 \alpha \times \frac{1}{\sigma T} = \alpha T$$

Thermoelectricity: the basics

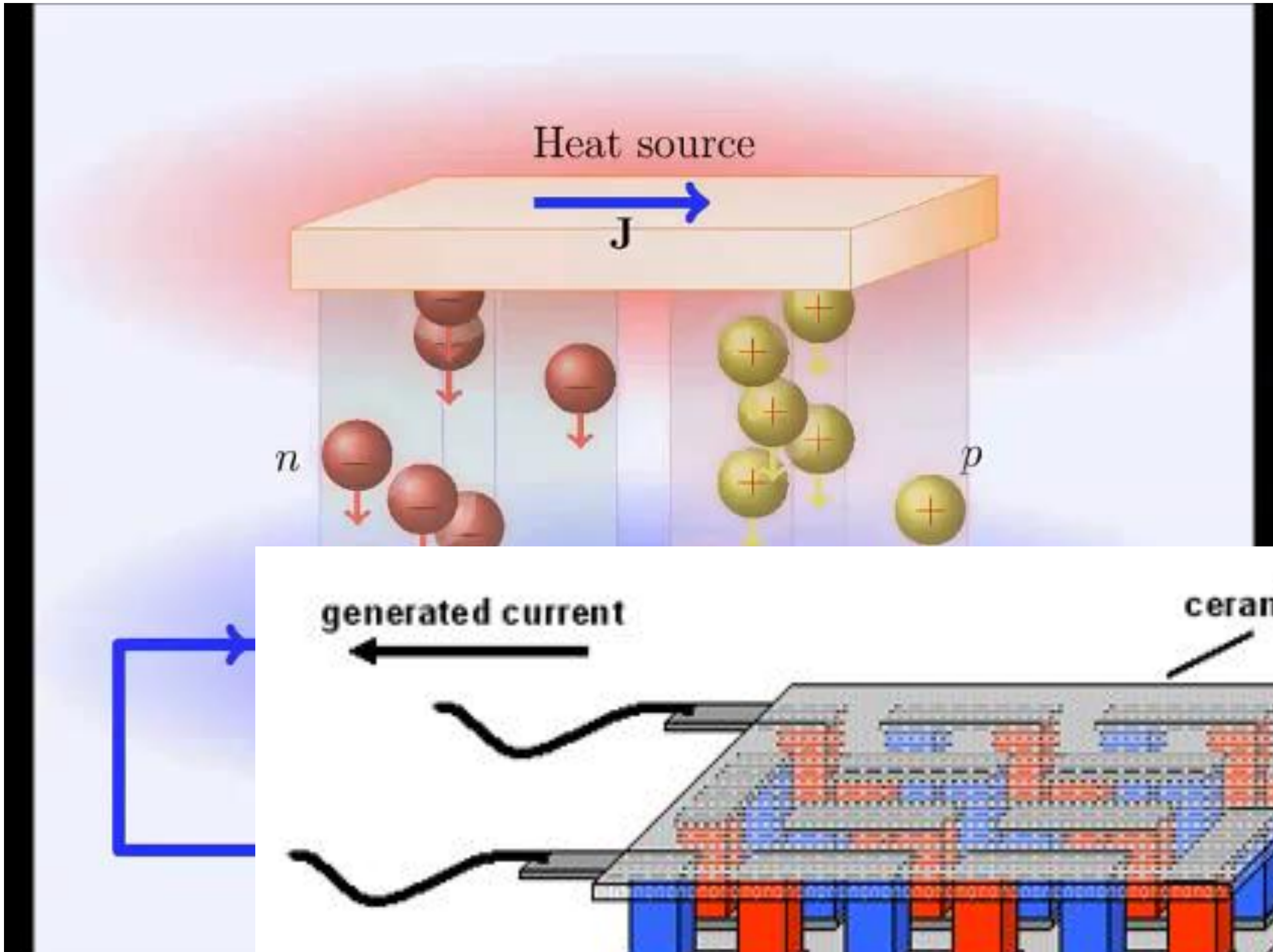

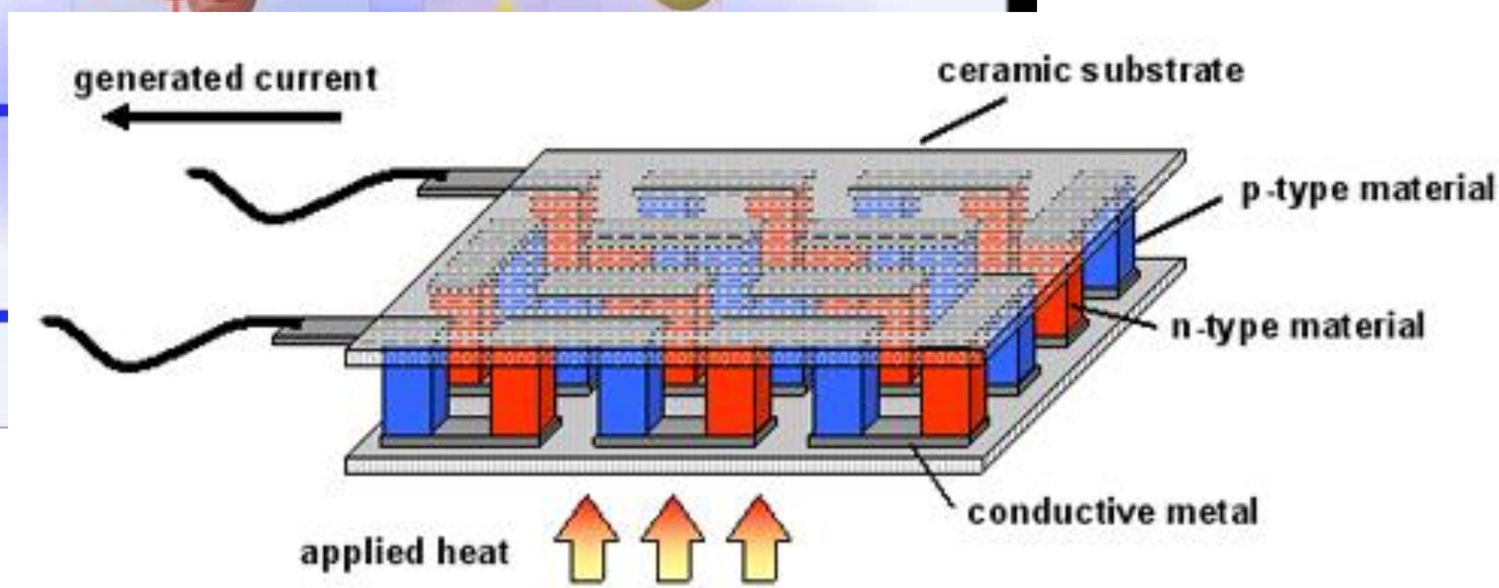

$$ZT = \frac{\sigma\alpha^2}{\kappa}T$$

Outline

- Why Heat Harvesting Matters
- Thermoelectricity: Physics and Technology
- **Materials Issues**
- Silicon as a New Player for Thermoelectrics:
    - SiGe alloys for RTGs
    - Si at low temperatures: Nanowires
    - Si at low temperatures: Thin Films
- From Materials to Devices
- Applications
- Some Conclusions

The Materials Challenge

Good thermoelectrics require ‘miracle materials’, with large electrical conductivity, a low thermal conductivity, and a high Seebeck coefficient

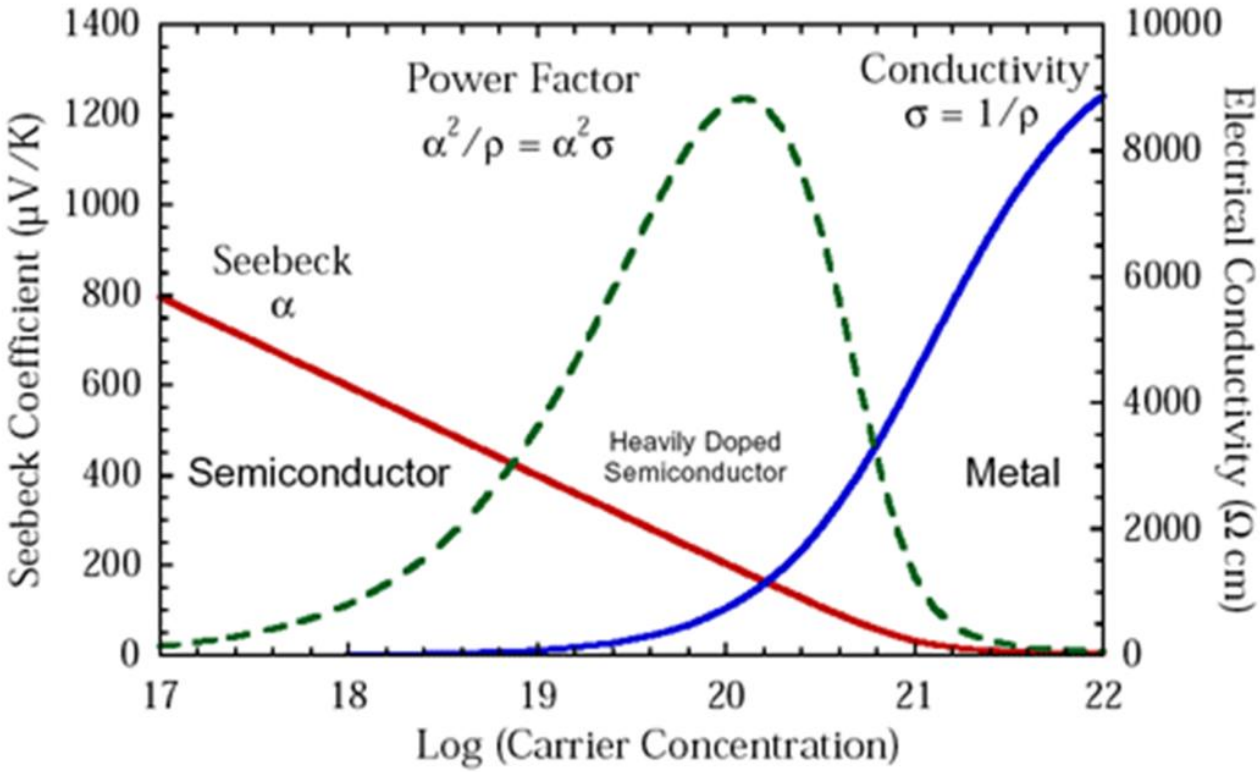

$$ZT = \frac{\sigma\alpha^2}{\kappa}T$$

The Materials Challenge

Thermoelectrics must overcome the competition of standard heat engines but also of other energy harvesting devices

Pro's

- No moving parts
- High reliability & lifetime
- Can be miniaturized
- Efficient at low T

Con's

- Low efficiency
- Expensive

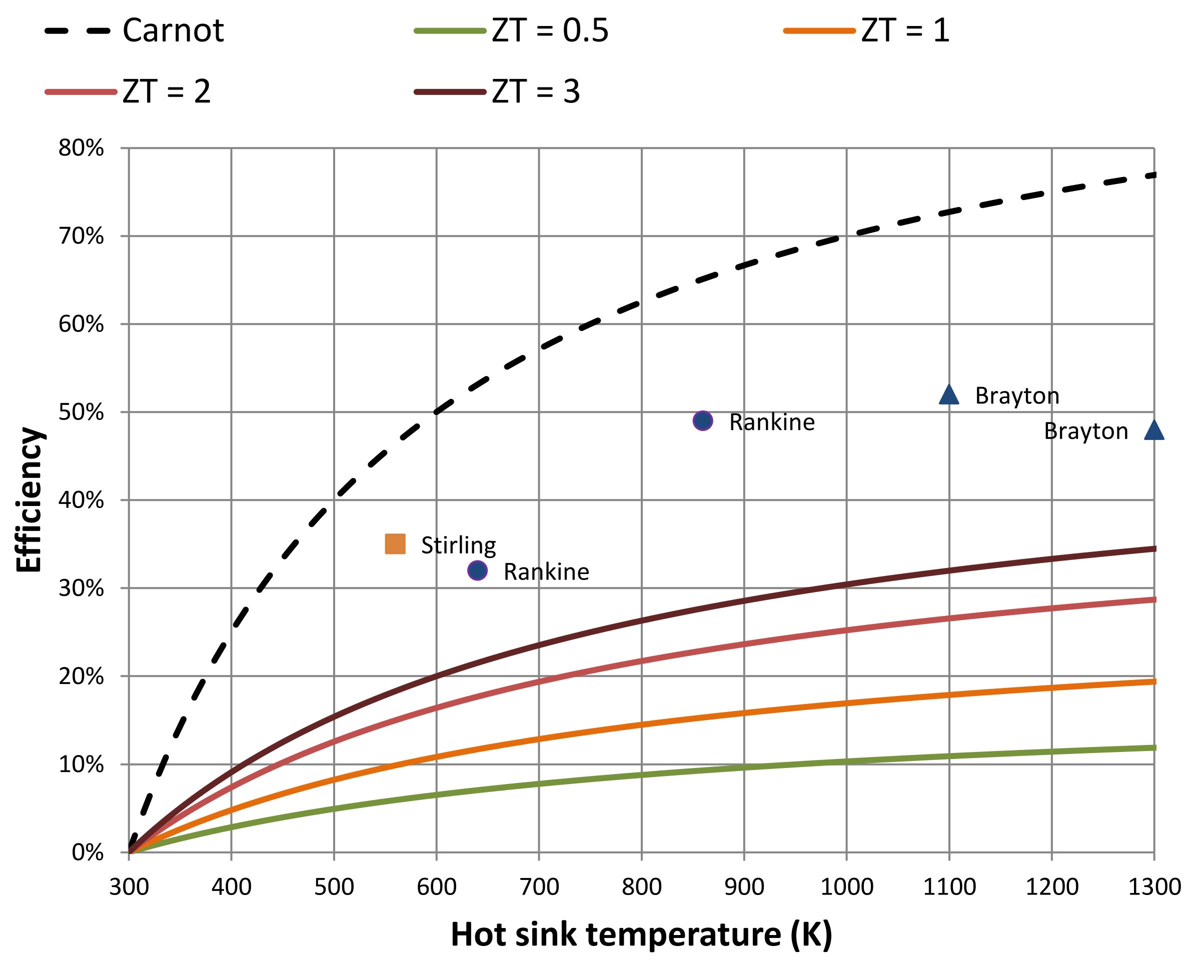

The Materials Challenge

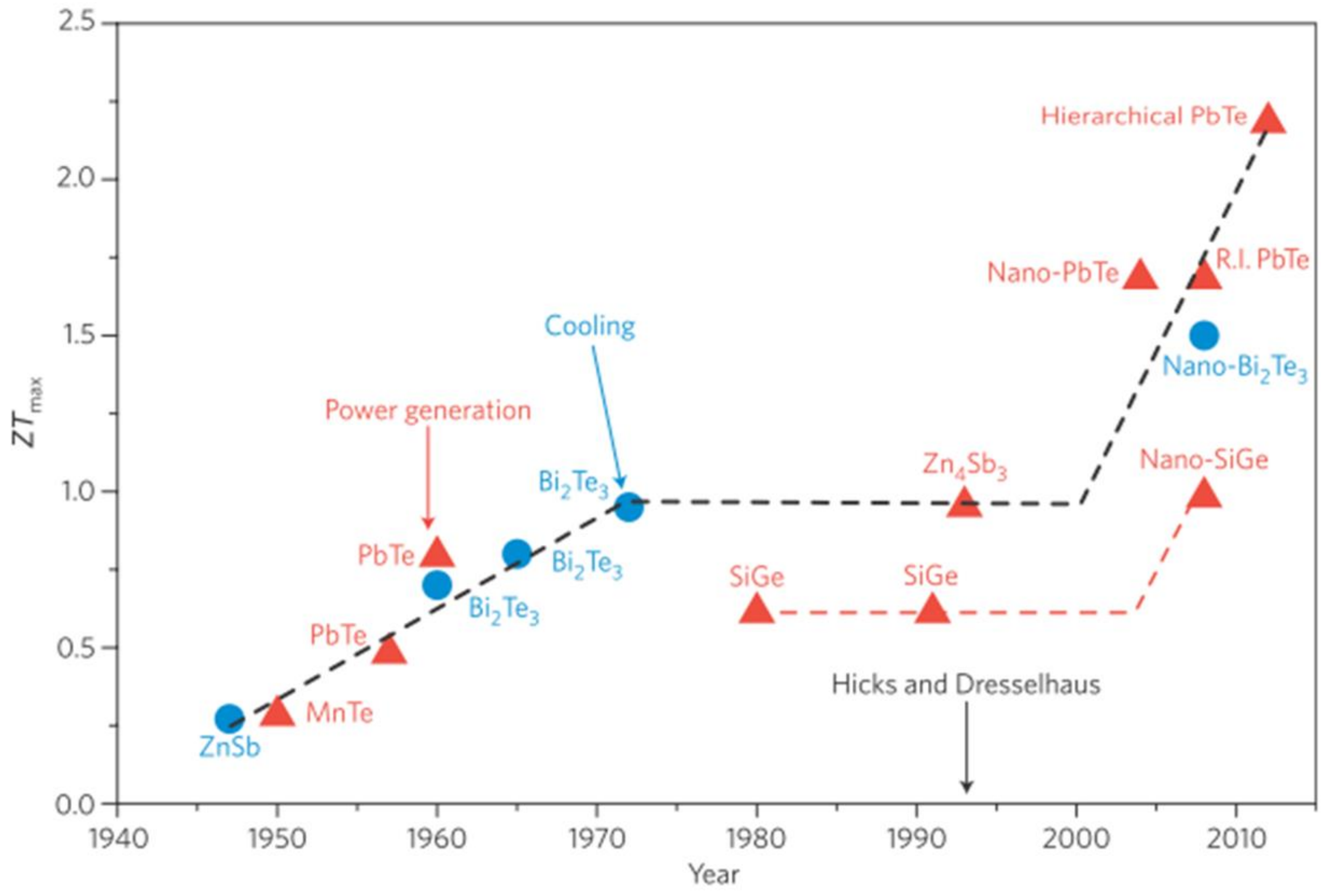

The Materials Challenge

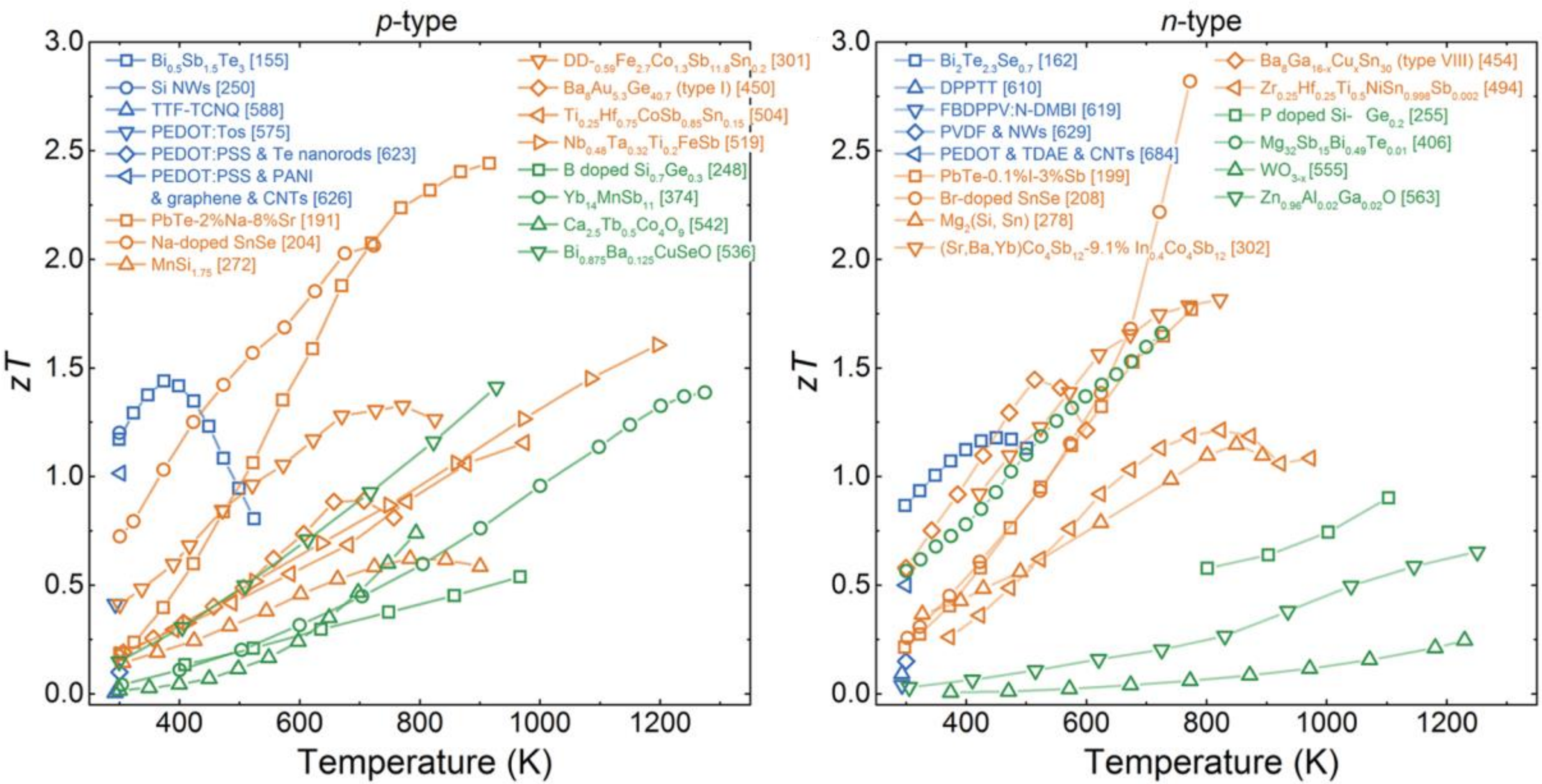

D. Beretta et al, Materials Science & Engineering R, 138 (2019) 210-255.

The Materials Challenge

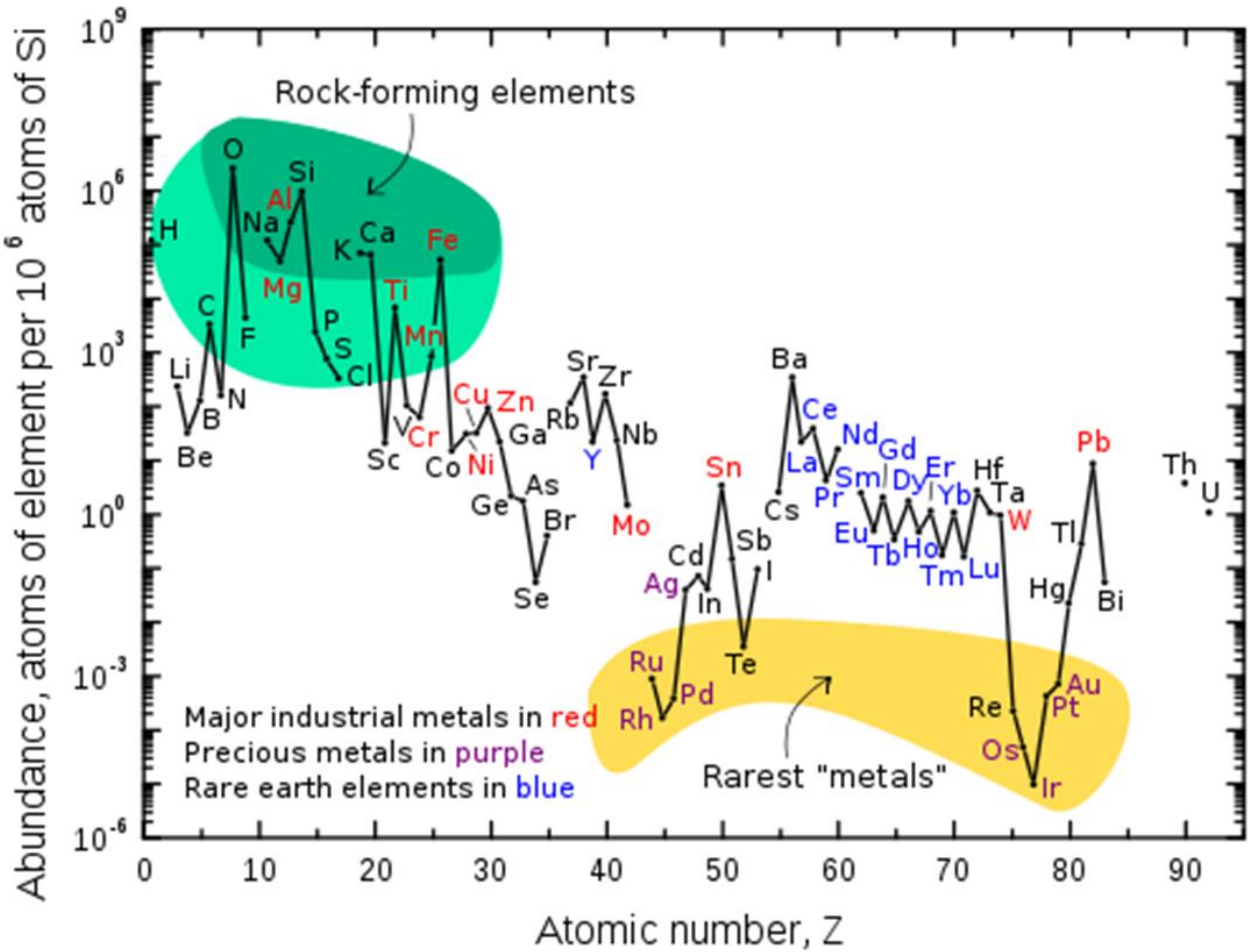

Outline

- Why Heat Harvesting Matters
- Thermoelectricity: Physics and Technology
- Materials Issues
- **Silicon as a New Player for Thermoelectrics**:
  - SiGe alloys for RTGs
  - Si at low temperatures: Nanowires
  - Si at low temperatures: Thin Films
- From Materials to Devices
- Applications
- Some Conclusions

Silicon as a New Player for Thermoelectrics

Strong need for largely geo-available TE materials operating around room temperature:

- heat body harvesting
- hybrid solar conversion
- cooling and heat management

Silicon (as SiGe alloys) seen in the past for high-temp applications.

Nanotechnology has shown instead its usability around room temp:

- Si nanowires
- Si nanopillars
- Si thin films

Si nanowires & thin films disclose power factors and ZT
fully comparable to tellurides, providing an IC-compatible, mature
and geo-abundant competitor

D. Narducci and F. Giulio, Materials, 15(3) (2022) 1214.

SiGe Alloys and Space Exploration

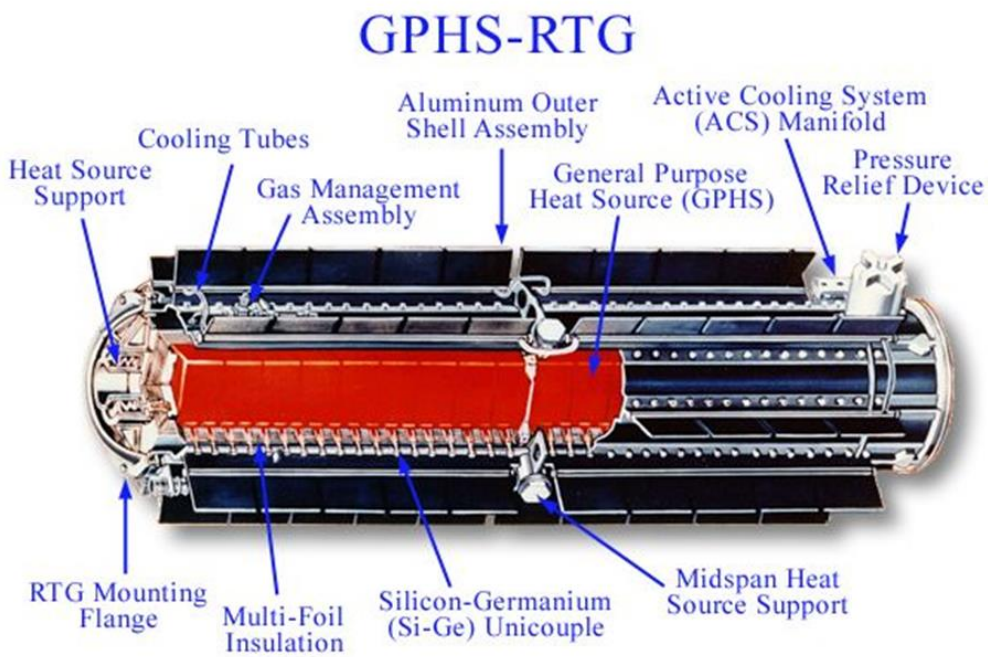

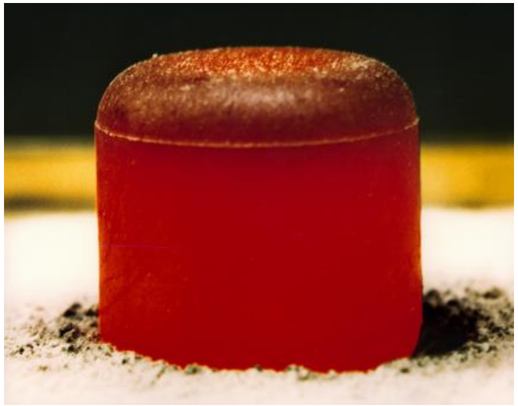

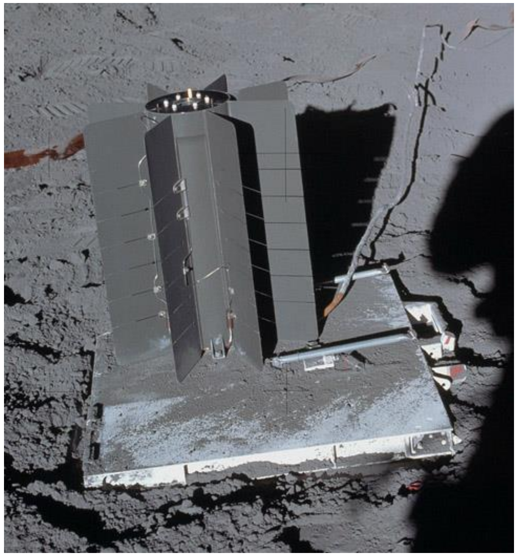

SNAP-27 on the Moon (Apollo 12)
70 W_e

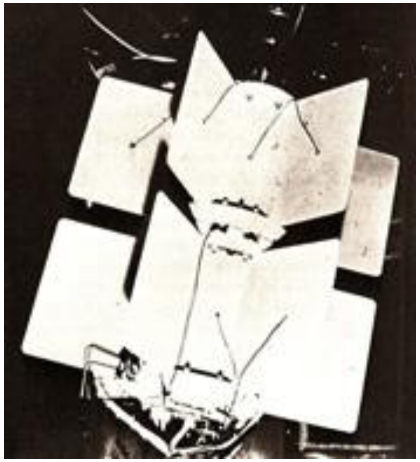

SNAP on Nimbus III (1968)
28.2 W_e

SiGe Alloys and Space Exploration

Pioneer 2 – Launched in 1972
RTEG still working in 2002 when leaving the solar system

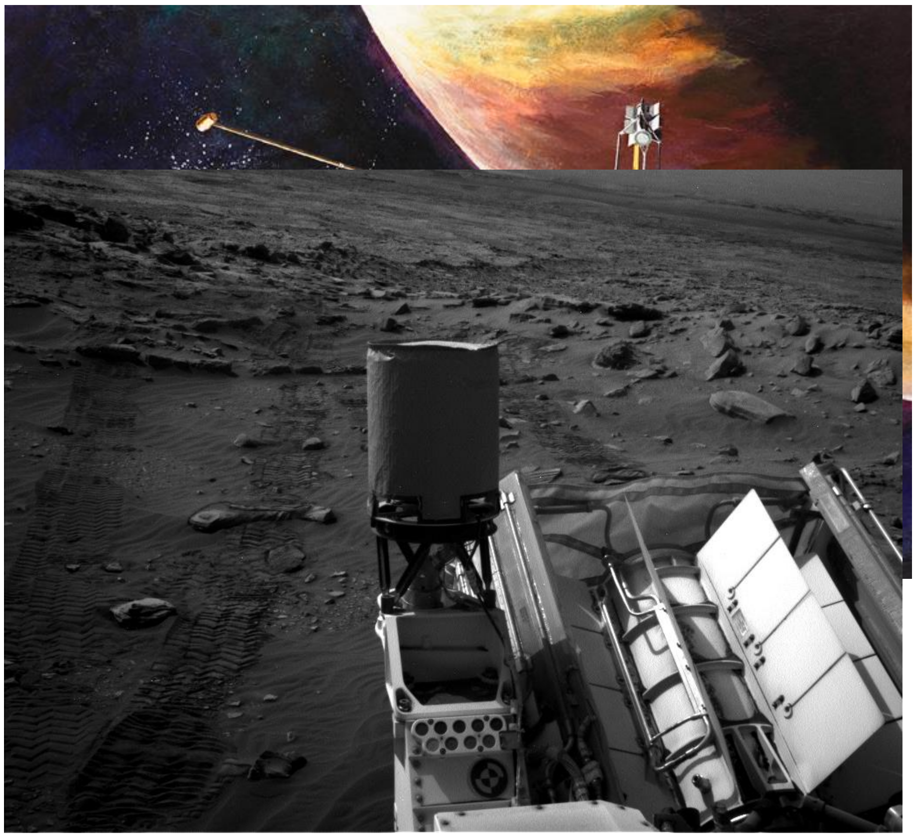

GPHS-RTG powering Curiosity
292 W_e

Silicon at Low Temperatures: Nanowires

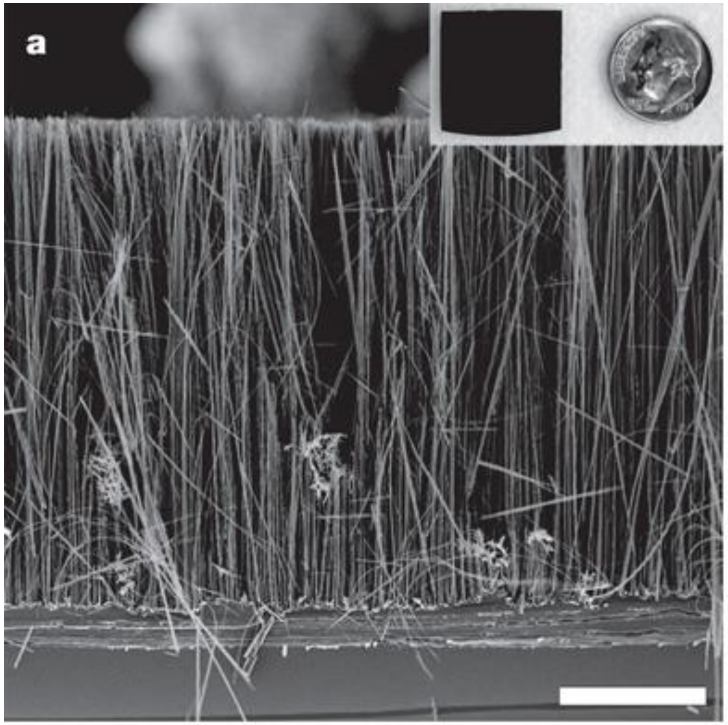

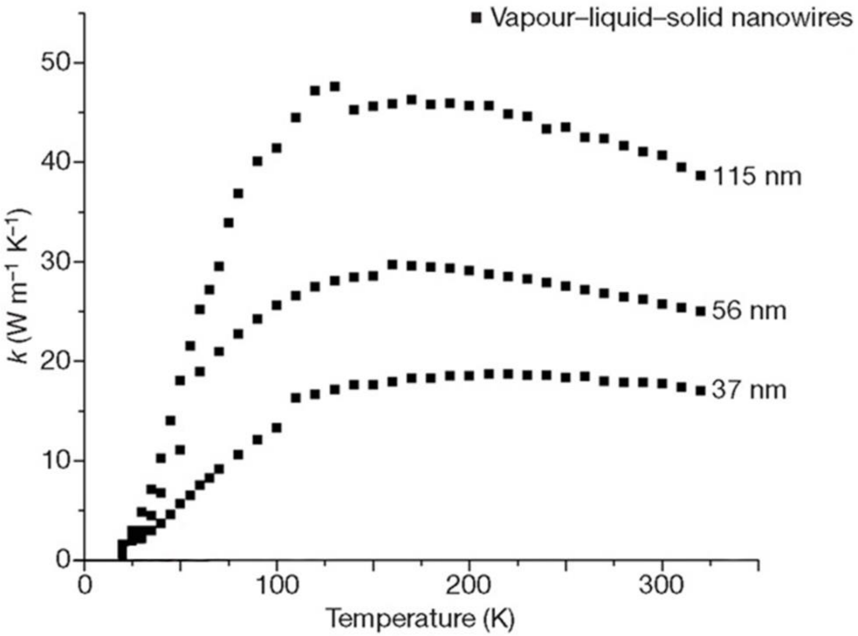

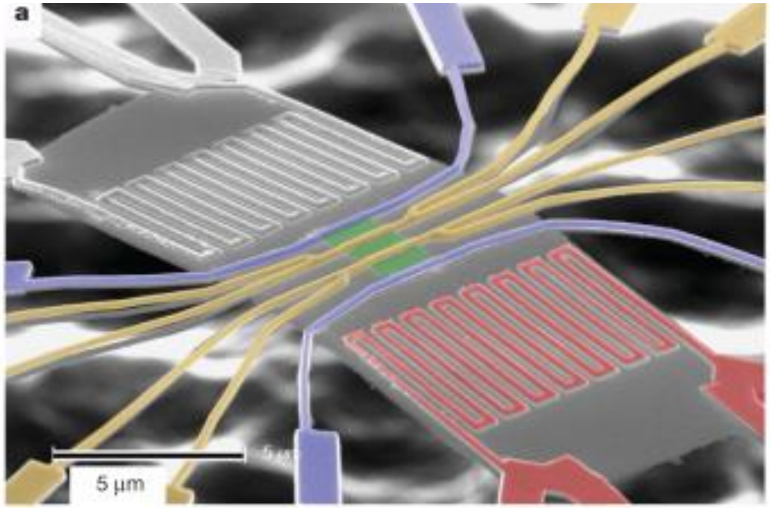

Incoherent phonon scattering along with coherent electron scattering at NW walls let σ/κ increase by two orders of magnitude

A.I. Boukai et al., Nature 451(7175), 168–171 (2008)
A.I. Hochbaum et al., Nature 451(7175), 163–167 (2008)

Silicon at Low Temperatures: Nanowires

Metal-Assisted Chemical Etching (MACE)

$$Ag^{+}_{(aq)} \rightarrow Ag_{(s)} + h^{+}$$

$$Si_{(s)} + 4h^{+} + 6H_2O_{(aq)} \rightarrow SiO_{2\,(s)} + 4H_3O^{+}$$

$$SiO_{2\,(s)} + 6HF_{(aq)} \rightarrow SiF_4^{2-}{}_{(aq)} + 4H_3O^{+}{}_{(aq)}$$

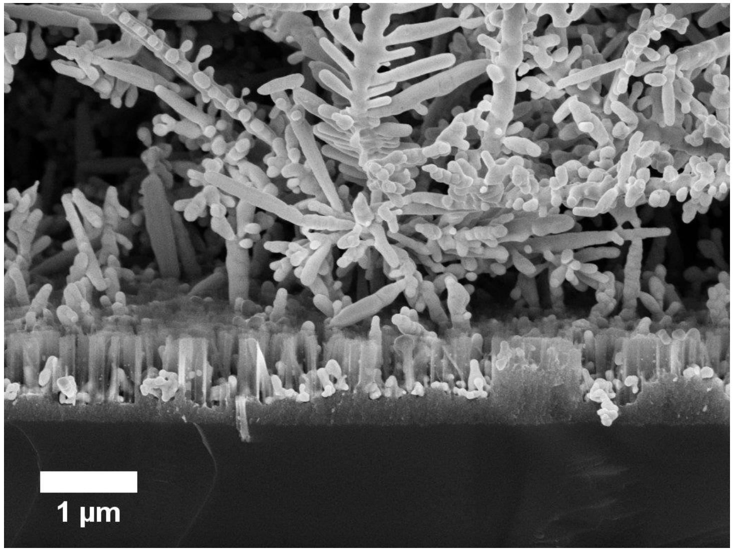

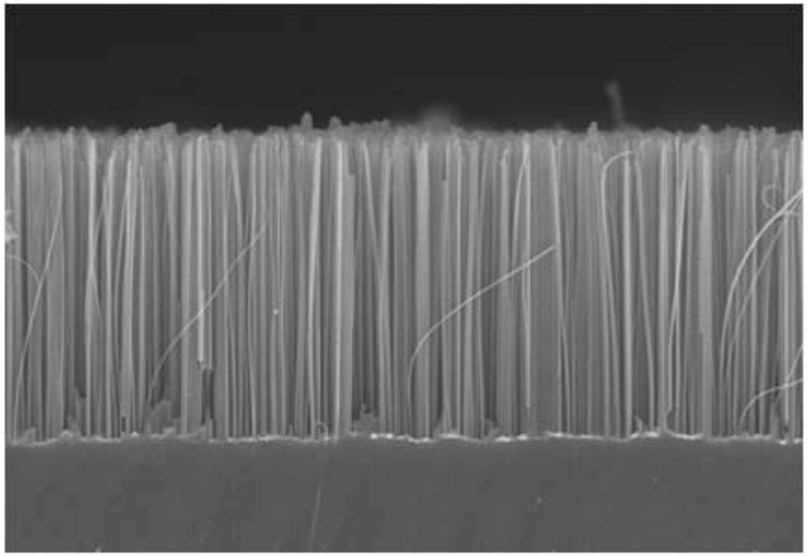

S. Magagna et al., Nanotechnology 31 (2020) 404002

Silicon at Low Temperatures: Nanowires

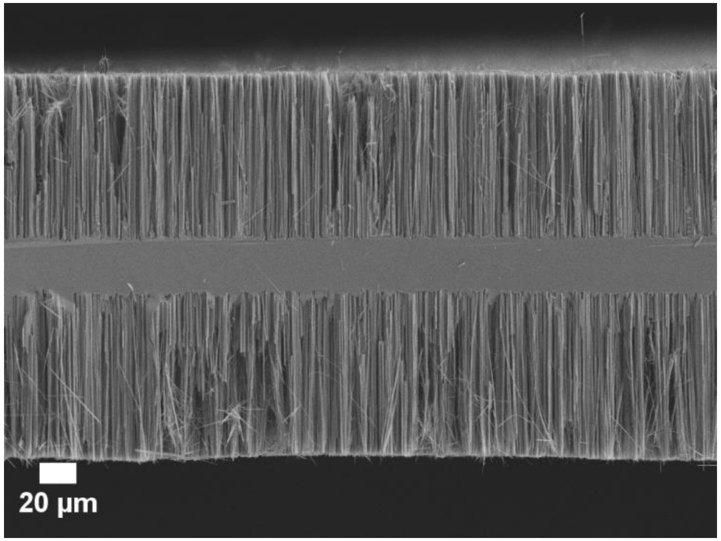

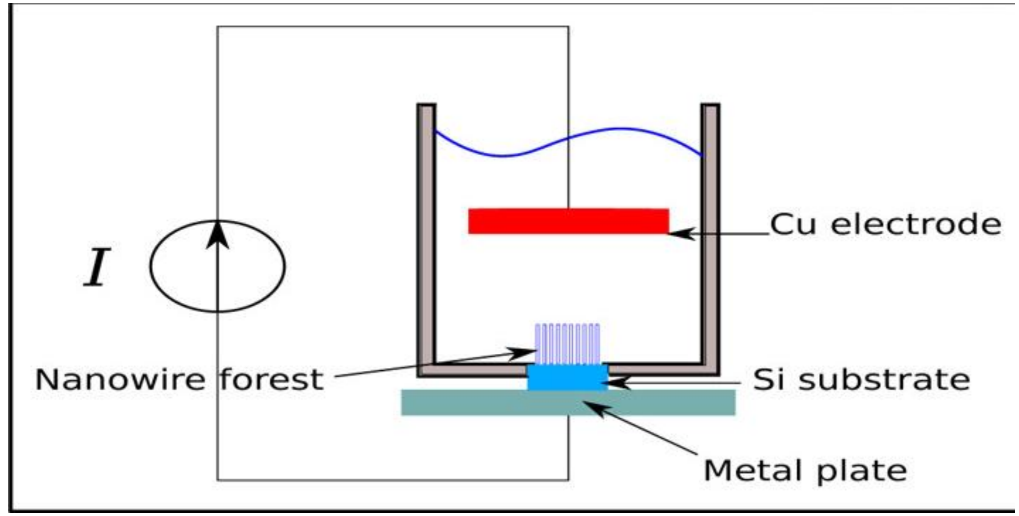

κ = 4.6 W/mK

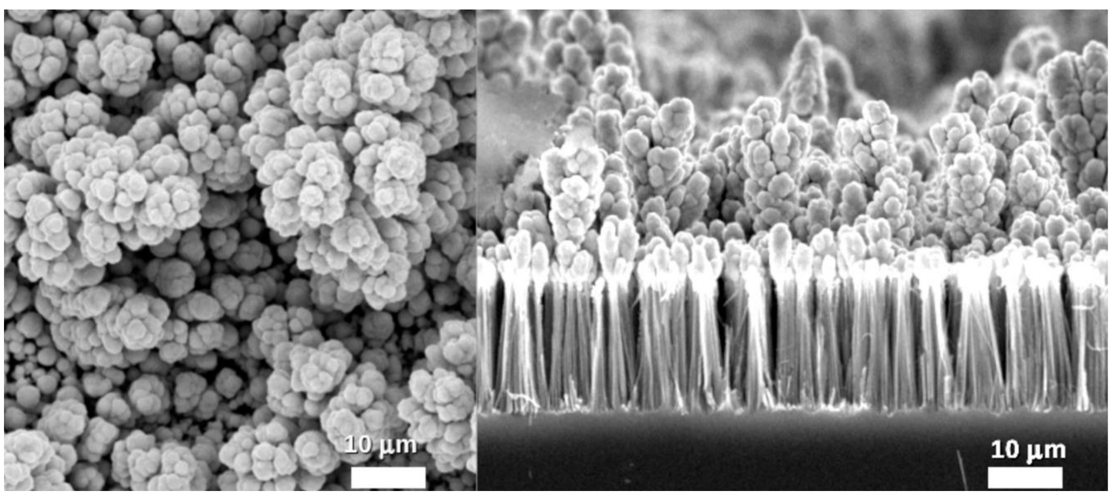

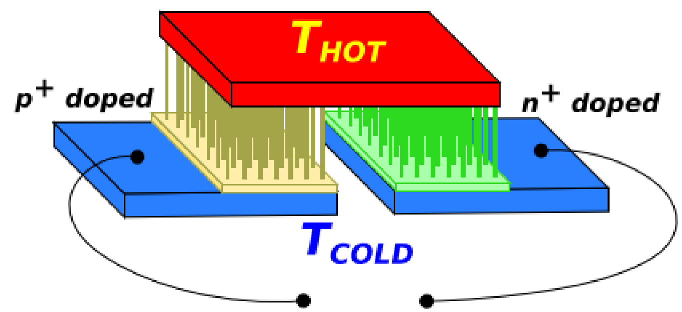

E. Dimaggio & G. Pennelli, Nano Letters 16 (2016) 4348
S. Elyamny et al., Nano Letters 20 (2020) 4748

Silicon at Low Temperatures: Nanowires

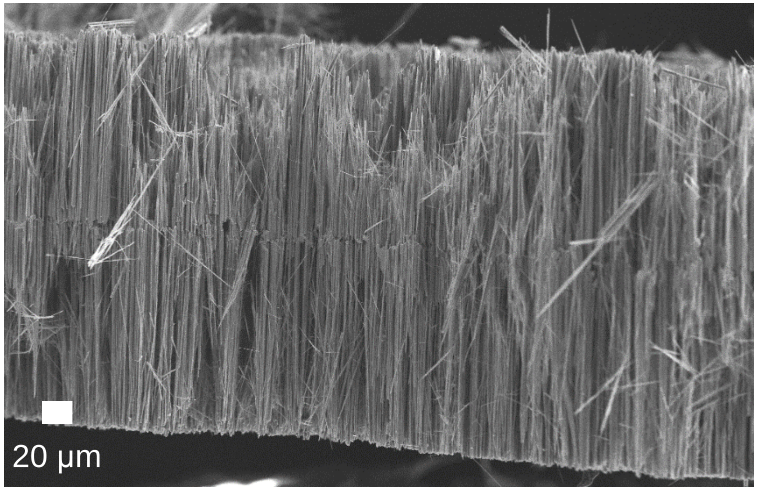

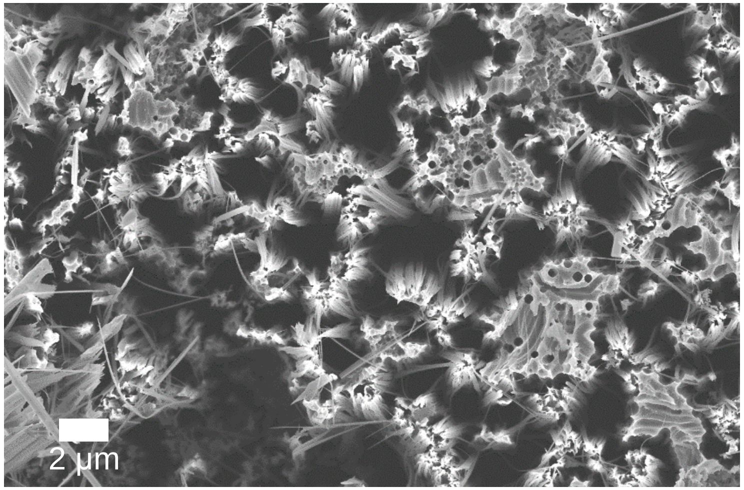

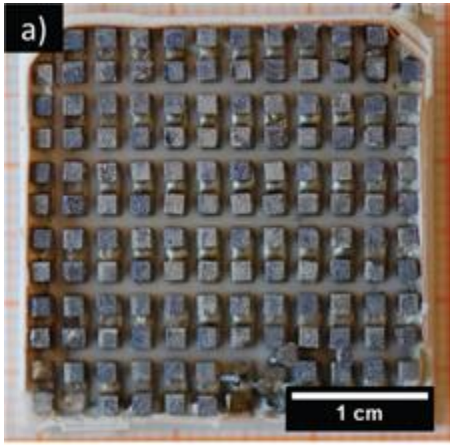

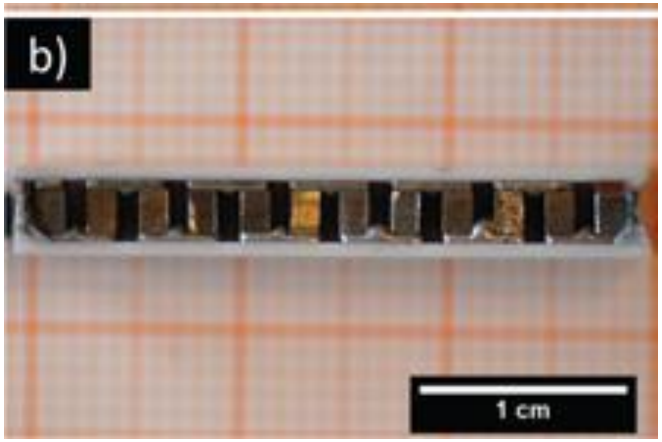

F. Giulio & D. Narducci, unpublished results

Silicon at Low Temperatures: Nanowires

B.L. Davis & M.I. Hussein, Phys. Rev. Lett. 112 (2014) 55505

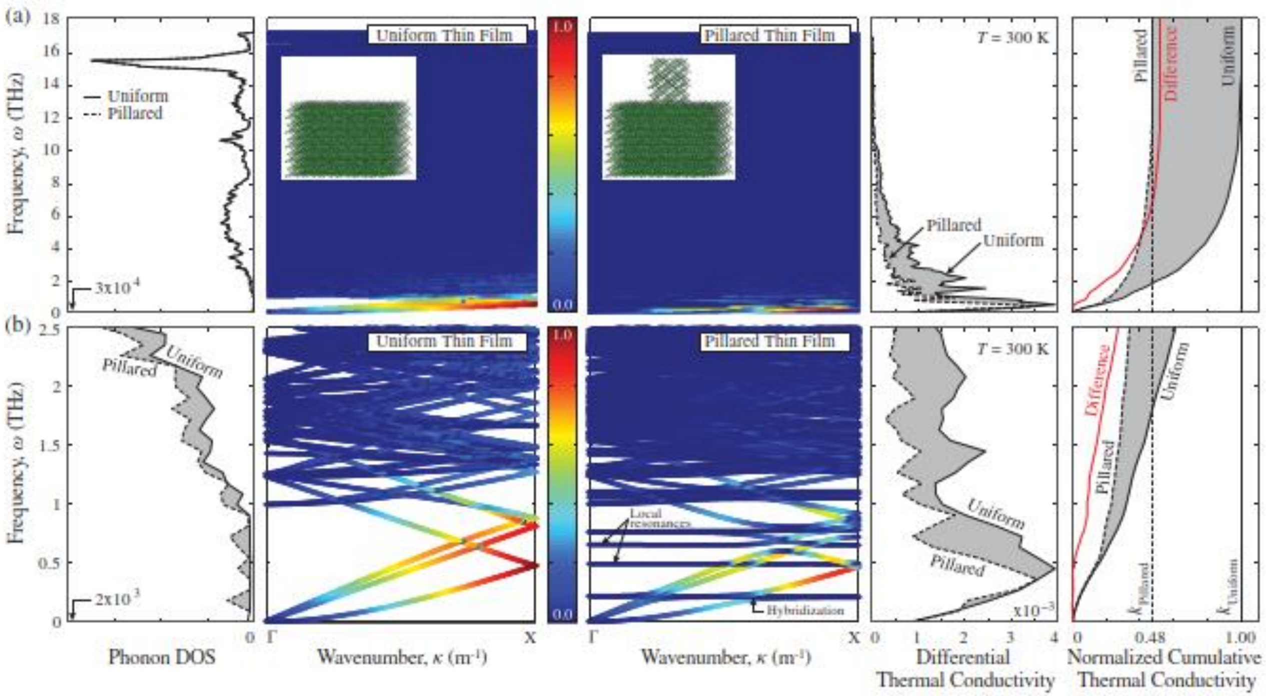

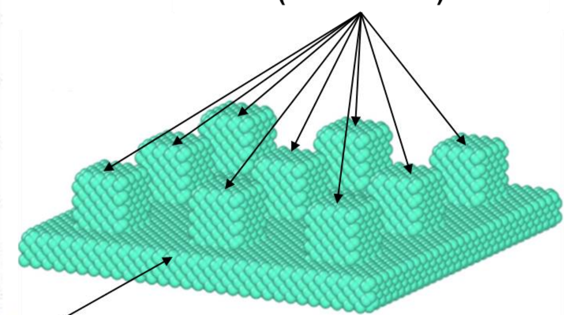

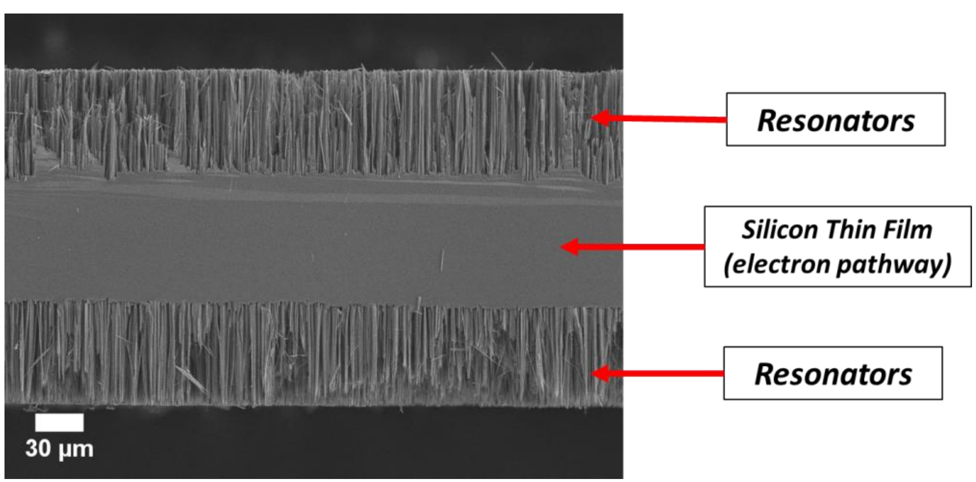

- σ and α of Si membrane (34 µm) unaltered
- κ of Si membrane reduced to 53 W/mK

S. Magagna & D. Narducci, unpublished results

Silicon at Low Temperatures: Thin Films

Films (220 nm) deposited by CVD at 625 °C using SiH_4 onto Si (100) | 100-nm SiO_x

Doping (4.4×10^{20} cm^{-3}) by I^2 (B^+, 26 keV, 6.0×10^{15} cm^{-2} + 47 keV, 6.0×10^{15} cm^{-2}), activated by RTP, 1050 °C, 40 s + thermal processing in Ar, 1000 °C, 2 hrs.

Above 800 °C, boron diffusivity is large enough to enable its migration, leading to its precipitation around GBs forming a B-rich second phase (possibly SiB_3).

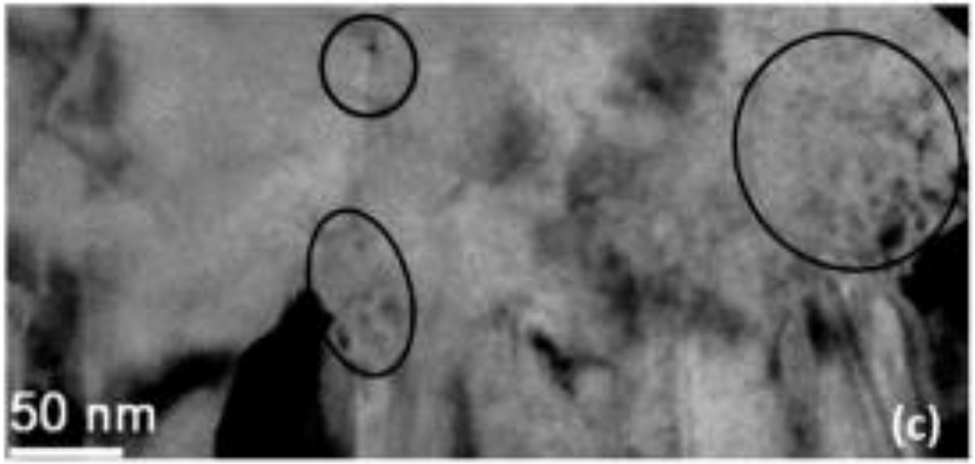

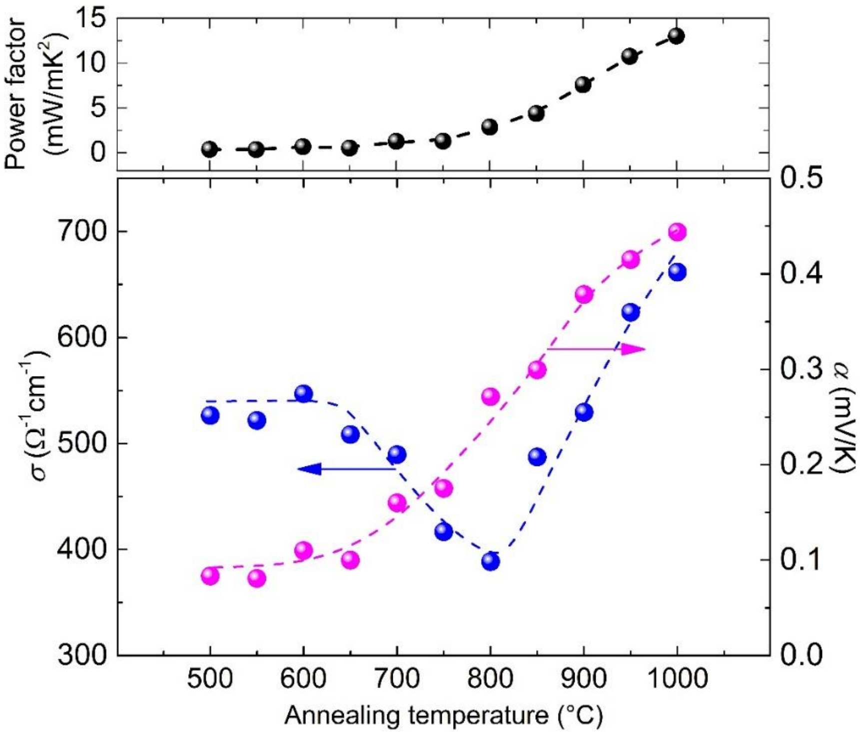

DN et al., Proc. 8th ECT, Como, 2010, 141
DN et al., J. Solid State Chem., 193 (2012) 19
DN et al., AIP Conf. Proc., 1449 (2012) 311
DN et al., Phys. Status Solidi A, 211 (2014) 1255
DN, S. Frabboni, X. Zianni, J. Mater. Chem. C, 3.47 (2015) 12176

Energy Filtering in nanoSi TFs

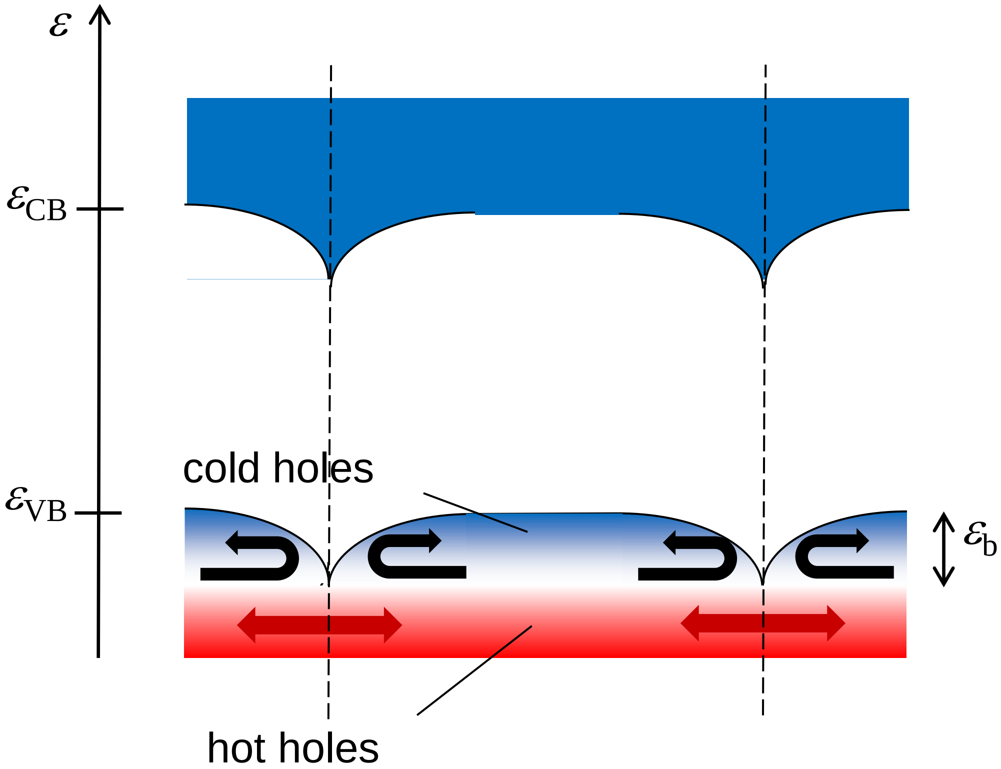

SiB_x sets barriers at GB

Cold holes are localized

Hole density decreases, so α increases

Since only hot holes diffuse, μ increases

The enhanced μ compensates for the reduction of p

The power factor increases

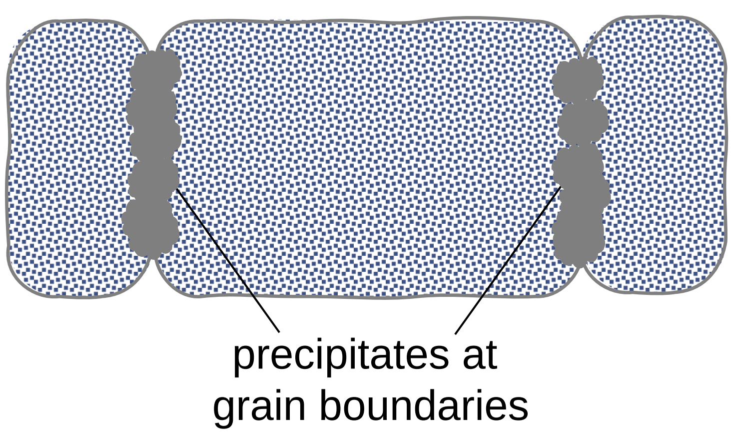

For the mechanism to be effective

- carriers must not relax within grains, so grain size must be ≈ MFP
- barrier height is critical

N. Neophytou et al., Nanotechnology, 24 (2013) 205402
N. Neophytou et al., J. Electron. Mater., 43 (2014) 1896
X. Zianni & D. Narducci, J. Appl. Phys., 117 (2015) 035102
X. Zianni & D. Narducci, Nanoscale, 11 (2019) 7667
N. Neophytou et al, Mater. Today Phys., 11 (2019) 100159

The Role of Hydrogen

- H remains embedded upon CVD growth
- H binds to B and dangling bonds at GBs
- Thus, H hampers B precipitation at GBs
- H presence confirmed by FTIR, with thermal processing causing its release
- Size effects in desorption processing reported, due to gas velocity at film surface

$$BH_4 \rightleftharpoons BH_3 + H_{Si}$$

$$H_{Si} \Rightarrow H_{surface}$$

$$2\ H_{surface} \rightleftharpoons H_{2\ surface}$$

$$H_{2\ surface} \rightleftharpoons H_{2\ gas}$$

Gas desorption depends on H_2 pressure nearby the film surface

V.F. Solovyov et al., Physica C 353 (2001) 14

The Role of Hydrogen

- Sample aged at room temperature for 5 years

Type	σ	α	PF ... K)	Relative PF
Untreated, aged				0.69
Small, aged				23.0
Large, aged				10.5

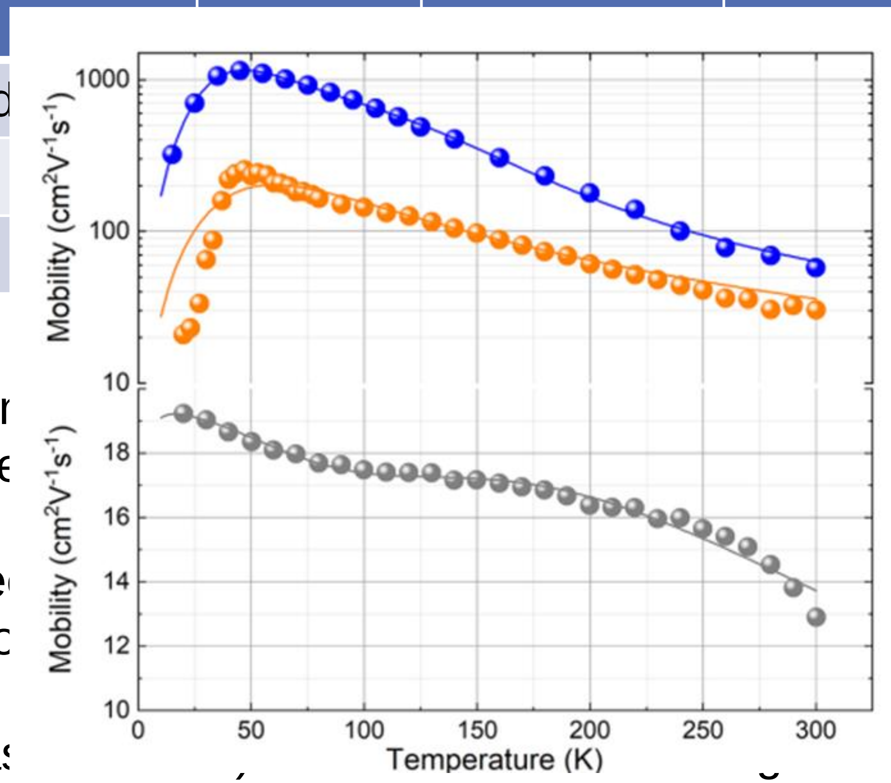

- Hydrogen had tir ... itions and at room temperature inde
- Partial spontane ... of thermal treatments (yet depending c
- This confirms (as ... mples, still hydrogen is present in thin films
- A top PF value of 33.1 mW/mK^2 was measured

Outline

- Why Heat Harvesting Matters
- Thermoelectricity: Physics and Technology
- Materials Issues
- Silicon as a New Player for Thermoelectrics:
  - SiGe alloys for RTGs
  - Si at low temperatures: Nanowires
  - Si at low temperatures: Thin Films
- **From Materials to Devices**
- Applications
- Some Conclusions

From Materials to Devices: Reliability

- Thermal contacts rule the actual amount of ΔT sensed by the TE legs
- In contacts to soft surfaces, additional thermal resistances arise
- Furthermore, thermal cycling may cause interdiffusion at metal-TE contacts
- Reliability issues often related to metallurgy

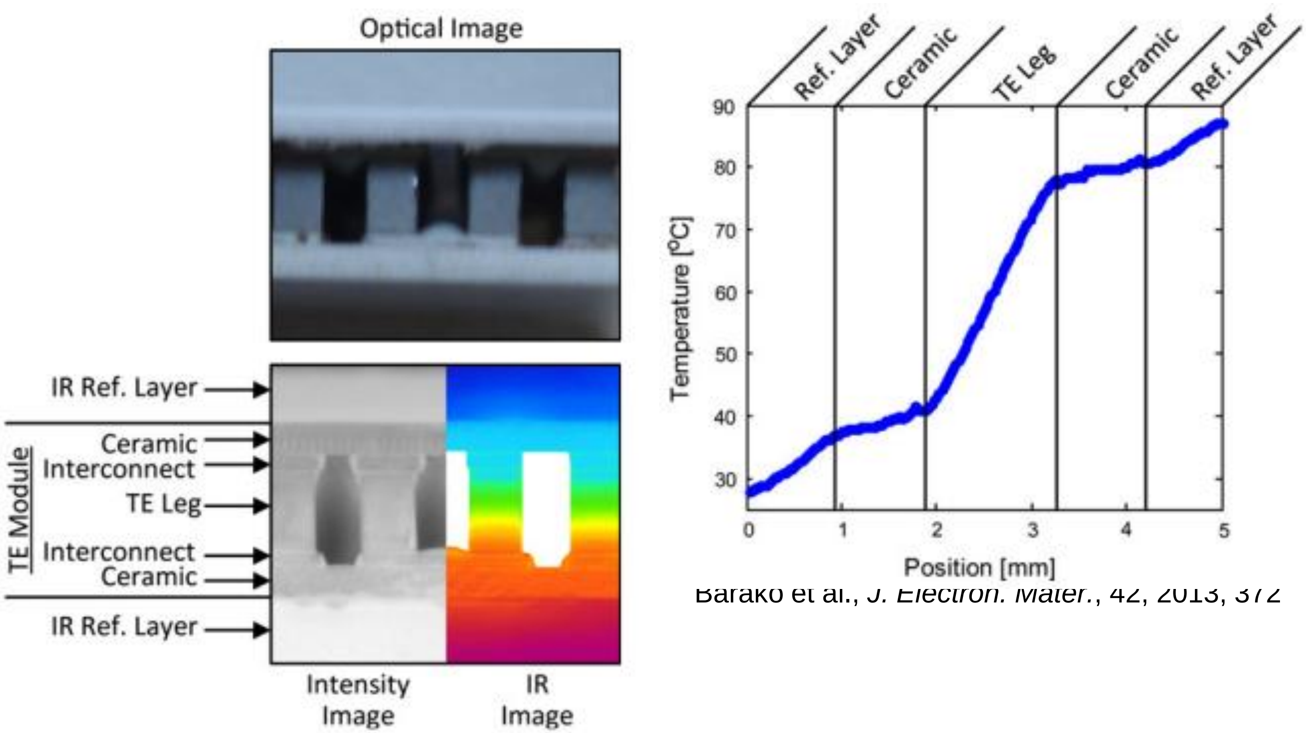

Barako et al., J. Electron. Mater., 42, 2013, 372

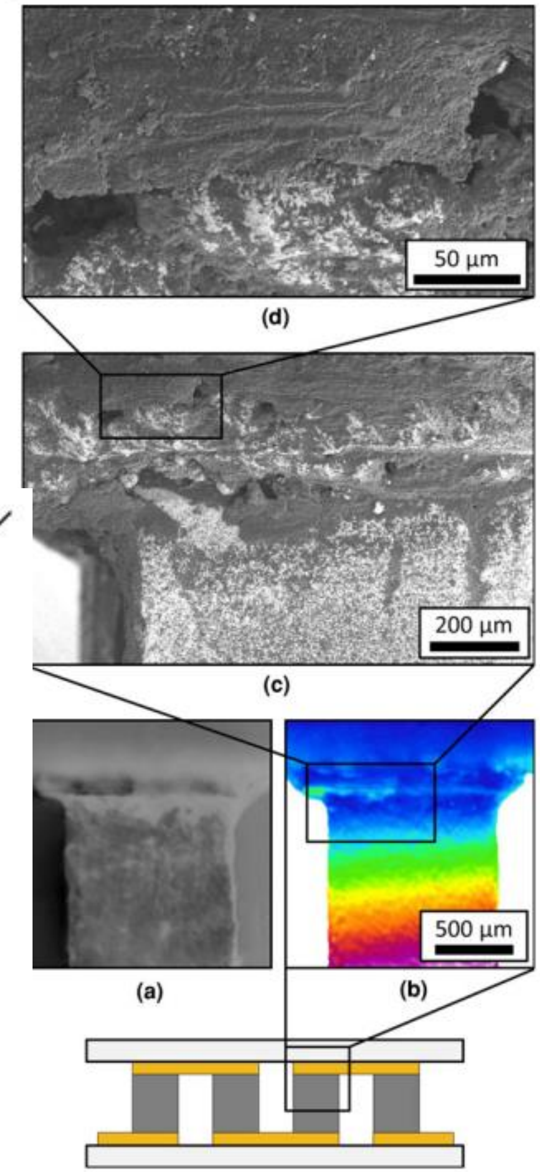

From Materials to Devices: Reliability

Low thermal conductivity causes large temperature *gradients* to develop for any given heat flux

This often enhances issues related to different CTE of materials, including interface stress

W. Liu et al., Scripta Mater. 111, 3 (2016)

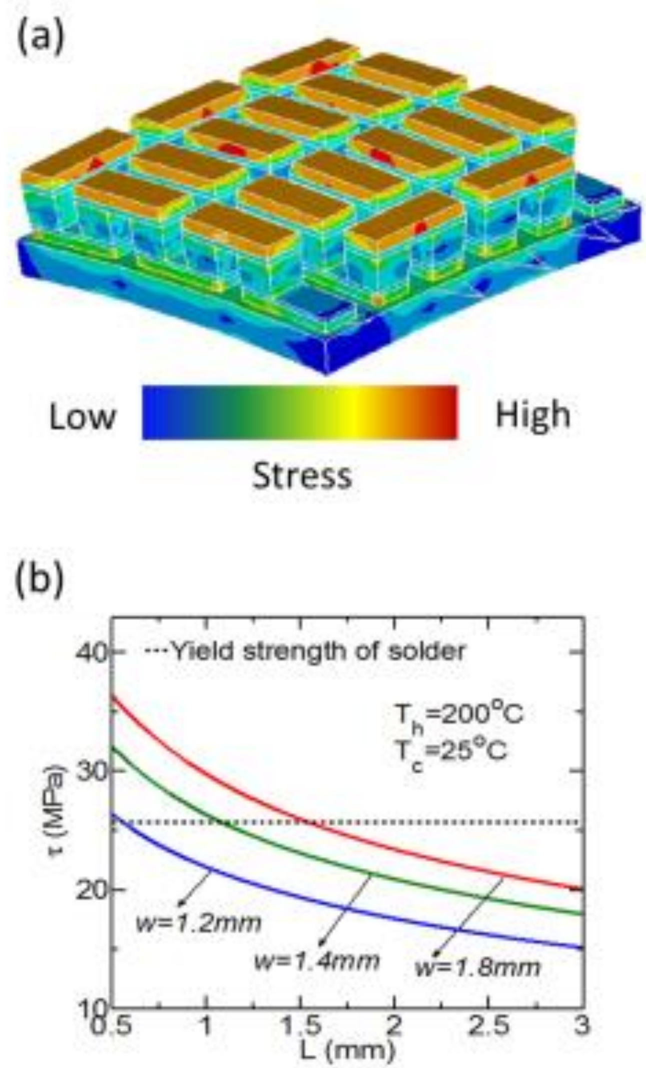

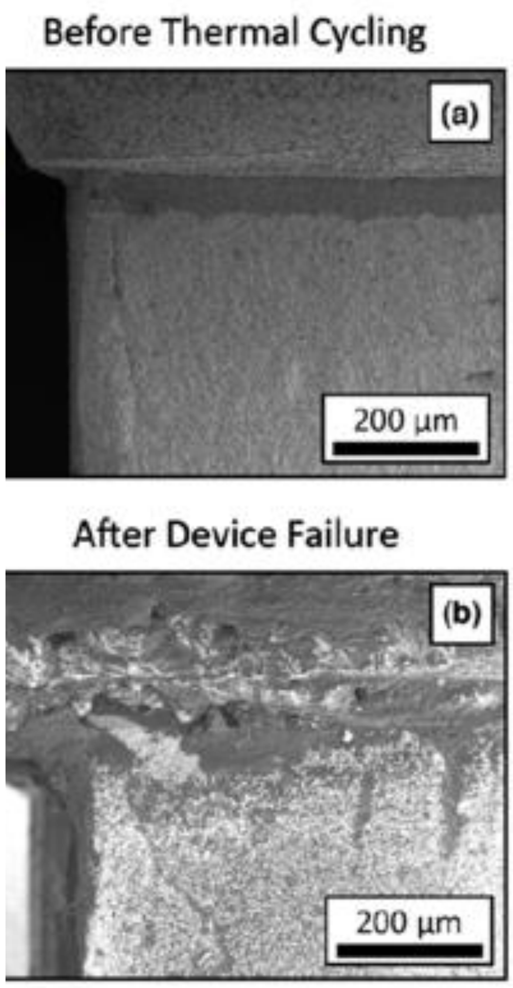

Outline

- Why Heat Harvesting Matters
- Thermoelectricity: Physics and Technology
- Materials Issues
- Silicon as a New Player for Thermoelectrics:
  - SiGe alloys for RTGs
  - Si at low temperatures: Nanowires
  - Si at low temperatures: Thin Films
- From Materials to Devices
- **Applications**
- Some Conclusions

Applications

RTG for *pacemakers* (USA, 1974)

emp scavenger (USA, 1974)

Watch powered by body heat (Japan, 1998)

Car muffler scavenger (Europe, 2005)

Applications: Co-generation (HTEPV)

PV efficiency is mainly limited by:

- loss of photons with $v < E_g/h$
- thermalization of photons with $v > E_g/h$ (also degrading PV efficiency)
- recombination

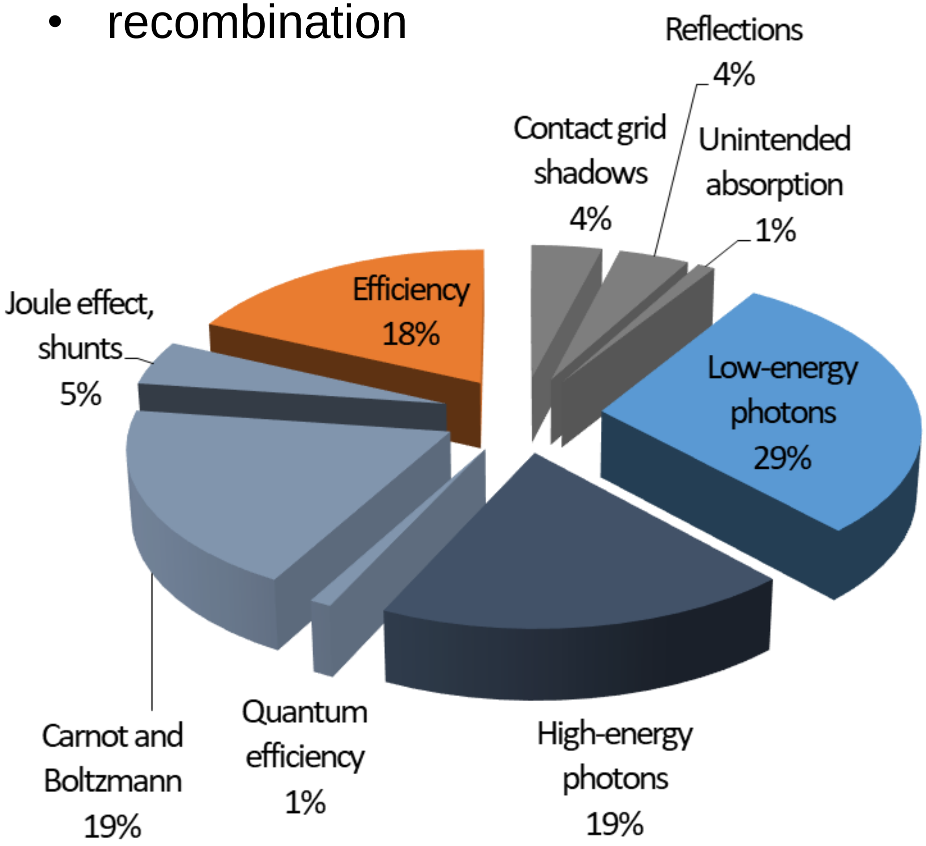

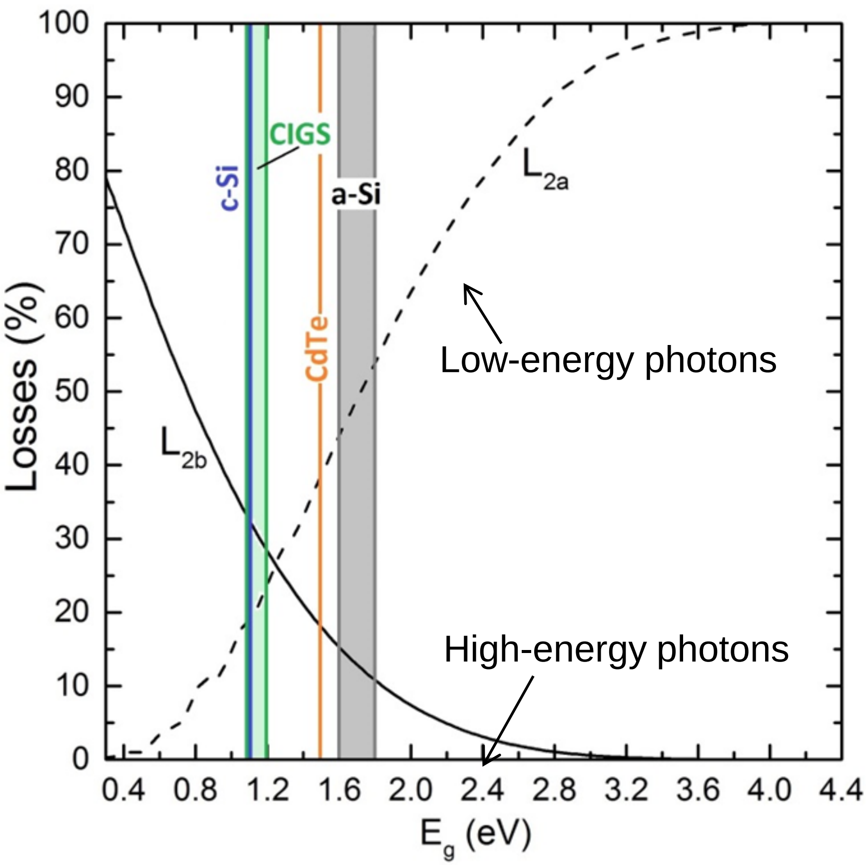

This mostly results in a production of heat that must be dissipated (to prevent η_{PV} degradation) but that might be also reused in TEGs

D. Narducci, P. Bermel, B. Lorenzi, N. Wang, and K. Yazawa, Hybrid and Fully Thermoelectric Solar Harvesting, (2018) Springer

Applications: Co-generation (HTEPV)

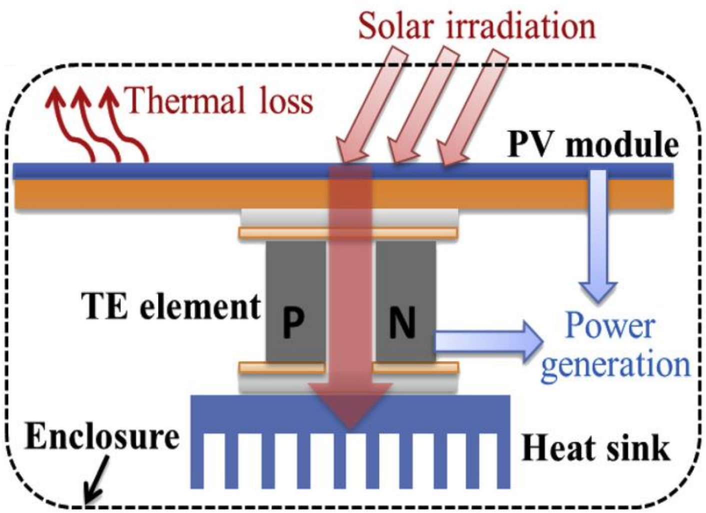

W. Zhu et al., *Energy*, 100, 2016, 91.

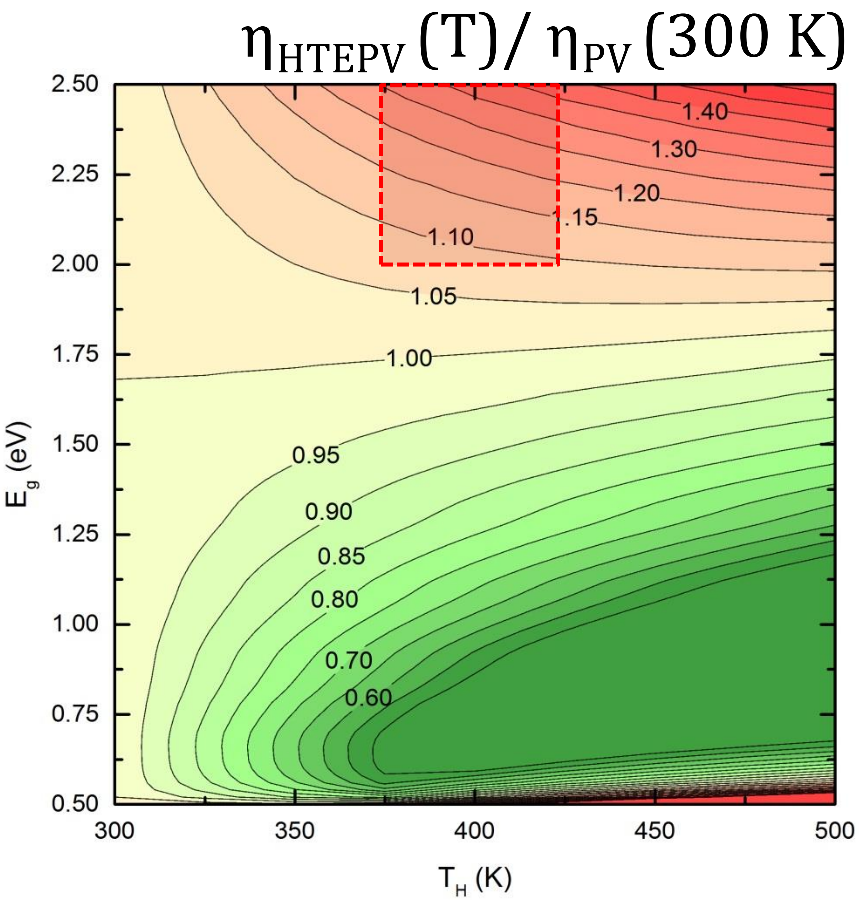

‘Upward’ reflective losses at PV surface
Heat mirror needed, transmitting radiation above the gap and backreflecting in the IR region.

Typical HM materials are oxides (TCO, ITO, etc.)

B. Lorenzi & G. Chen, J. Appl. Phys., 124 (2018) 024501

B. Lorenzi et al., J. Electron. Mater., 44 (2015) 1809
B. Lorenzi et al., J. Mater. Res., 30 (2015) 2663

Applications: Co-generation (HTEPV)

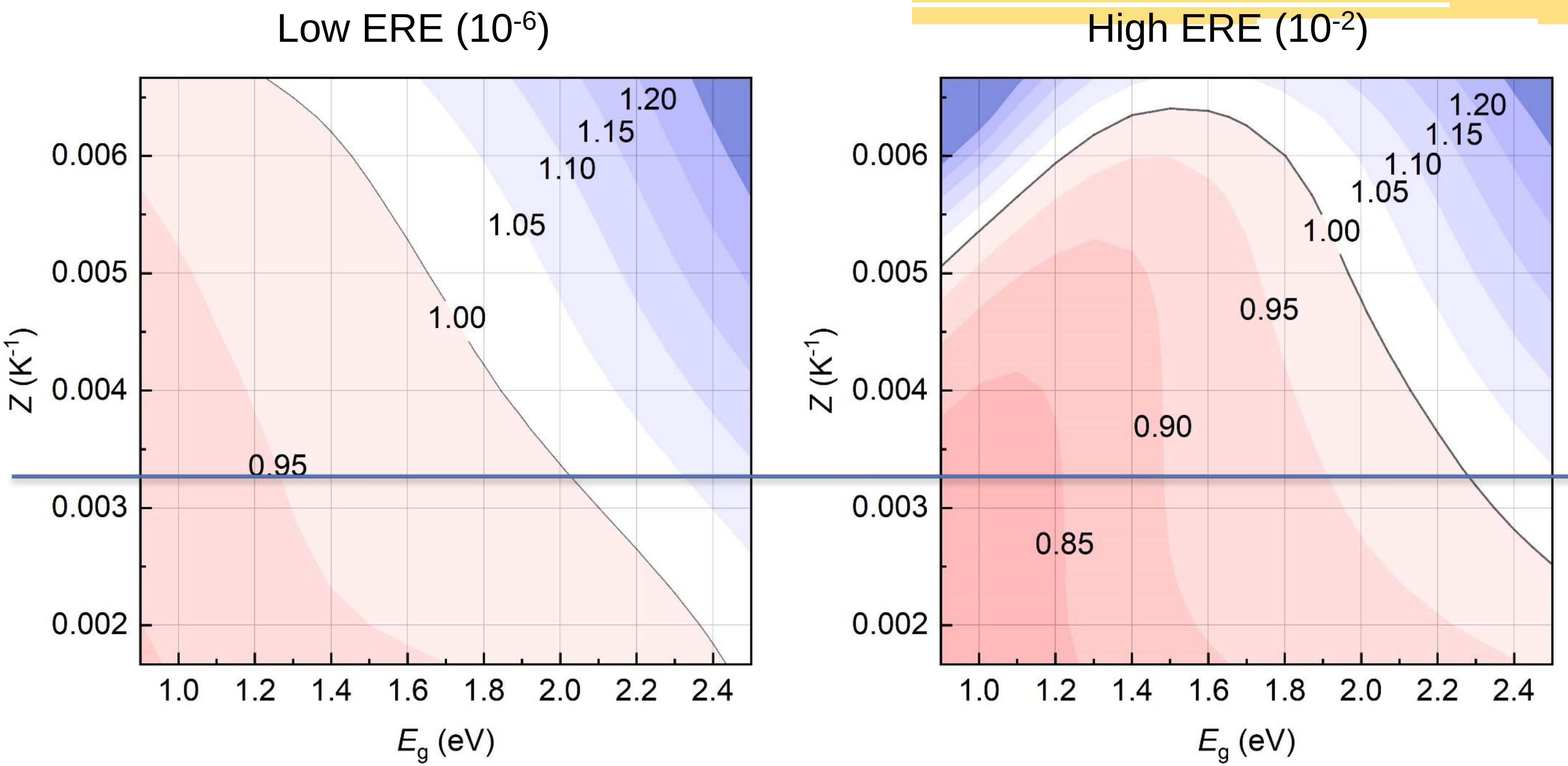

Economic analysis shows that

- neither concentrated or moderately concentrated HTEPVs are profitable for $zT \approx 1$ and E_g in the standard range 0.8-1.5 eV
- TE pairing with PV may be suitable to promote low-cost «poor» PV materials (such as a-Si, µc-Si:H)

D. Narducci , B. Lorenzi, ACS Appl. Energy Mater. 2021, 4, 4, 4029–4037

Applications: Co-generation (HTEPV)

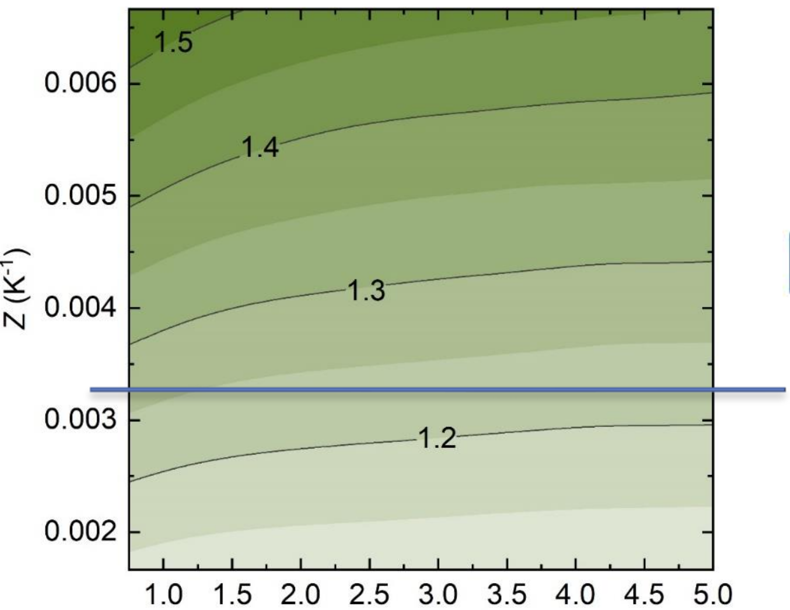

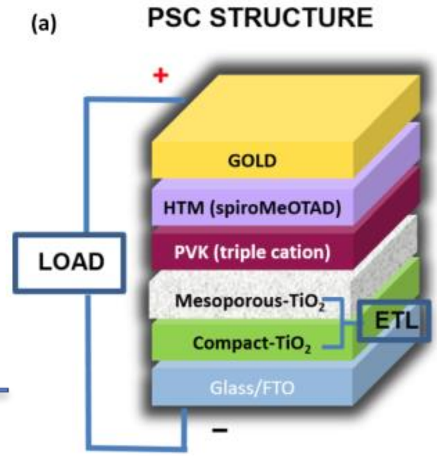

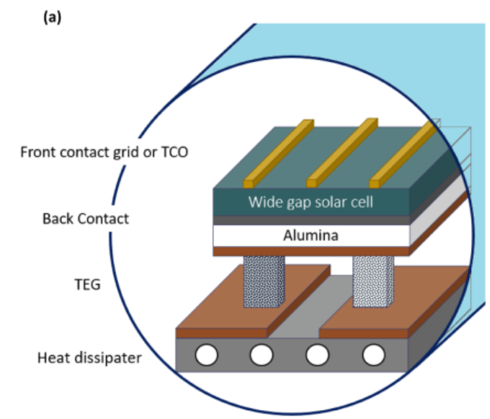

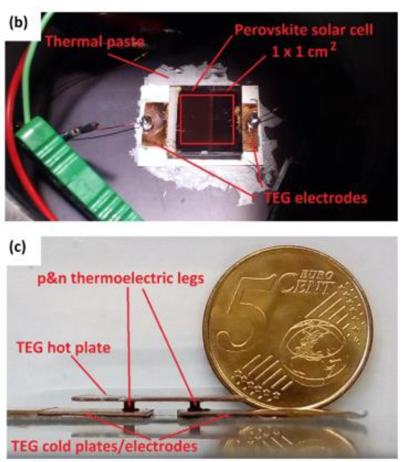

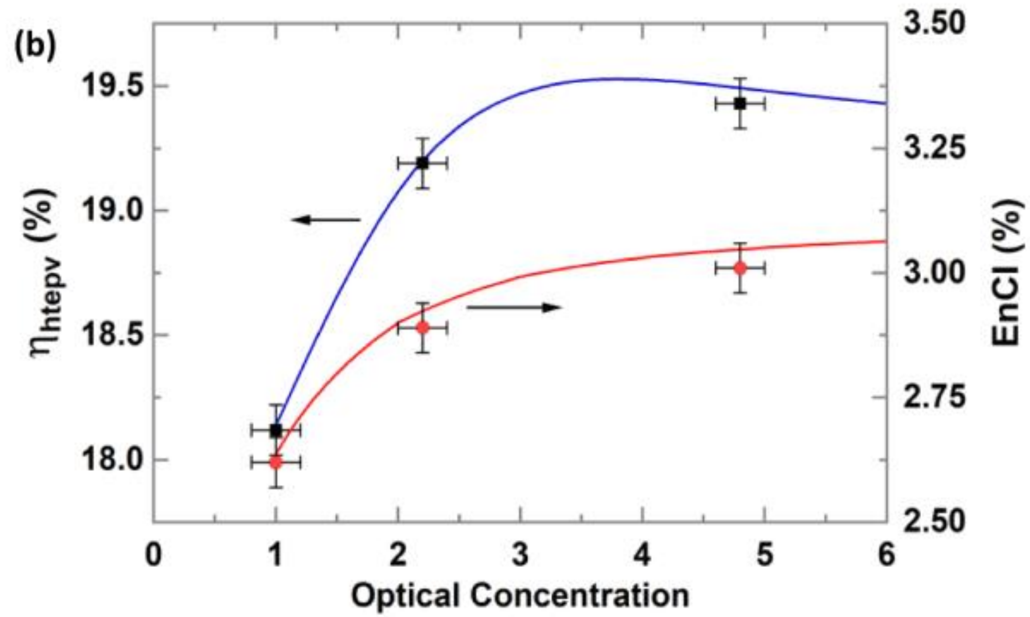

B. Lorenzi et al., Applied Energy, 300, 2021, 117343

Applications: Microgeneration

In 2006, devices autonomously exchanging information have outnumbered humans connected to Internet worldwide.

IoT is often populated by remotely deployed devices, so that sensing nodes need not only to exchange data wirelessly but also to operate maintenance-free over their lifetime.

Either energy sources or renewable energy converters must be then embedded in the sensor.

Applications: Microgeneration

TEG competition with batteries must be evaluated as of:

- energy requirements, comparing battery energy storage with energy demand of services sensing nodes
- power requirements, comparing the electric power a TEG can generate to the power demand of sensing nodes
- economic competitiveness, comparing power and energy costs of TEGs and batteries

D. Narducci, J. Phys.: Energy 1 (2019) 024001

Applications: Microgeneration

Cost models

Batteries

Type	Specific energy (J/g)	Specific Power (W/g)	Energy cost (USD/MJ)
Lead acid	134	0.18	40
NiCd	176	0.15	119
NiMH	305	0.5	119
NiZn	360	3.0	113
$LiCoO_2$	587	0.29	152
$LiFePO_4$	358	2.4	152

D.N., J. Phys.: Energy 1 (2019) 024001

TEGs

For bulk TEGs

- optimized power costs currently ≈ 38.5 USD/W
- device *costs* for commercial TEGs ≈ 5.6 USD (bulk *prices* ≈ 25 USD)

For microTEGs (MEMS cost model)

- devices costs depend on litho steps but ruled by packaging
- range from 1.03 USD/cm^2 (1L) to 1.48 USD/cm^2 (5L)
- estimated power costs from 60 USD/W (1L) to 120 USD/W (5L)

Applications: Microgeneration

Energy demand

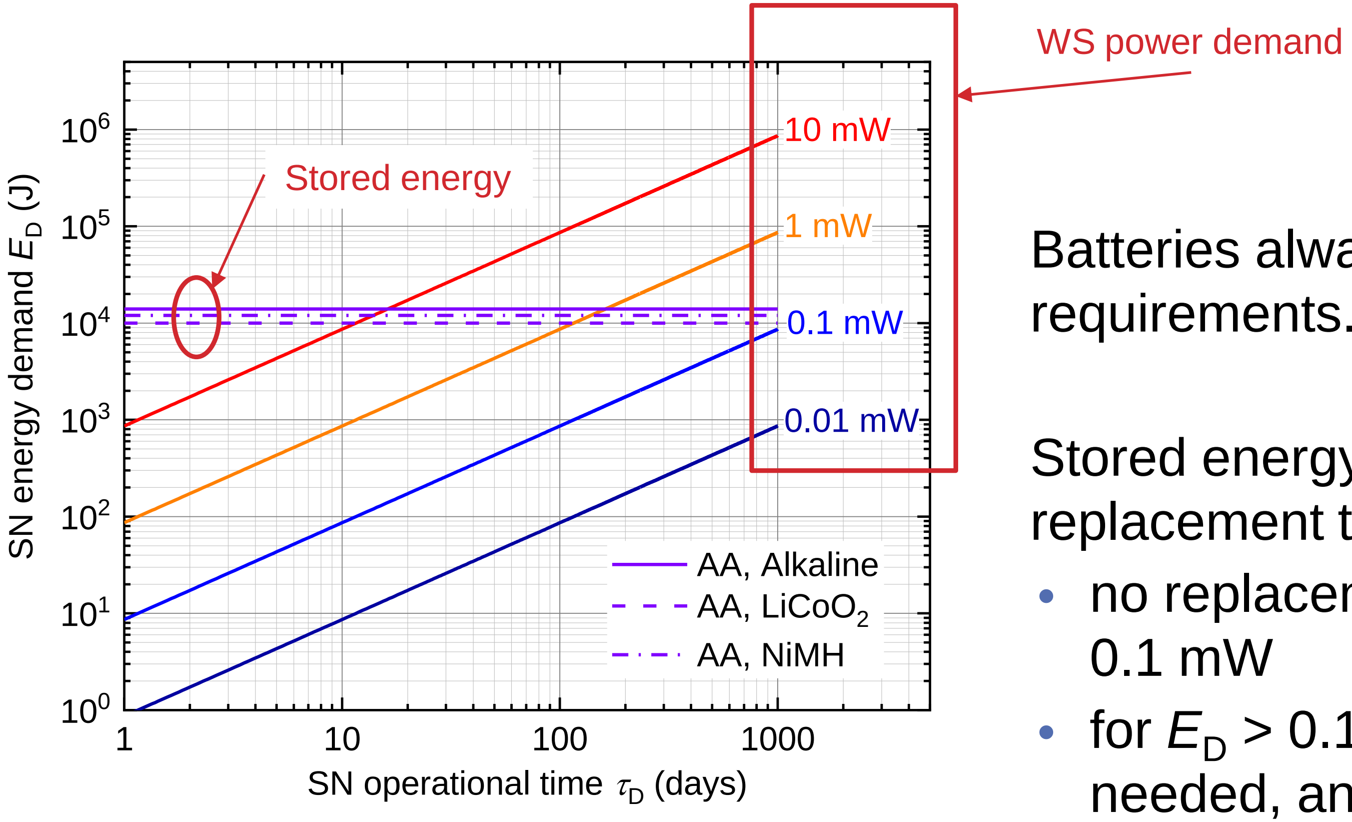

Batteries always meet *power* requirements.

Stored energy sets instead replacement times:

- no replacement needed for < 0.1 mW
- for E_D > 0.1 mW, replacements needed, and costs must be accounted for

Applications: Microgeneration

Power demand

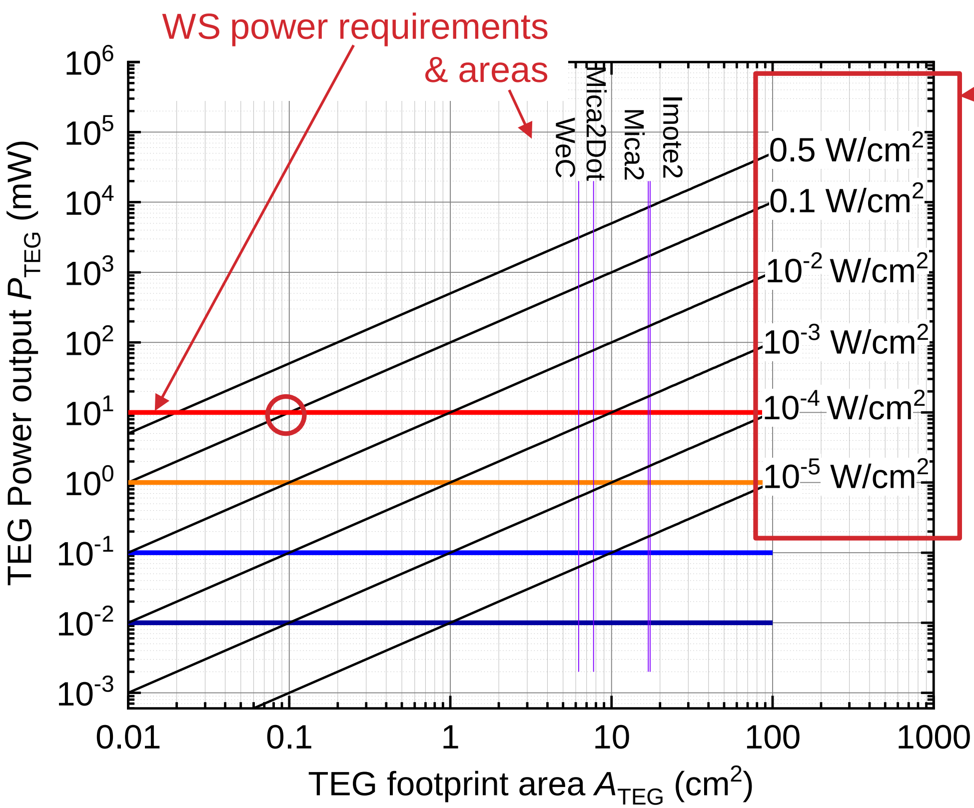

TEGs have no *energy* constraints, being harvesters

Cross-points set minimal TEG areas

- MicroTEGs may service WSs with power demands < 0.1 mW only
- Bulk TEGs provide enough power to suit any WSs, even when accounting for thermal chain inefficiency/lower ΔT

Power limitations for TEGs are therefore less stringent than possibly expected. Competitiveness is set by economic factors.

Comparison: Powering costs

Powering Costs

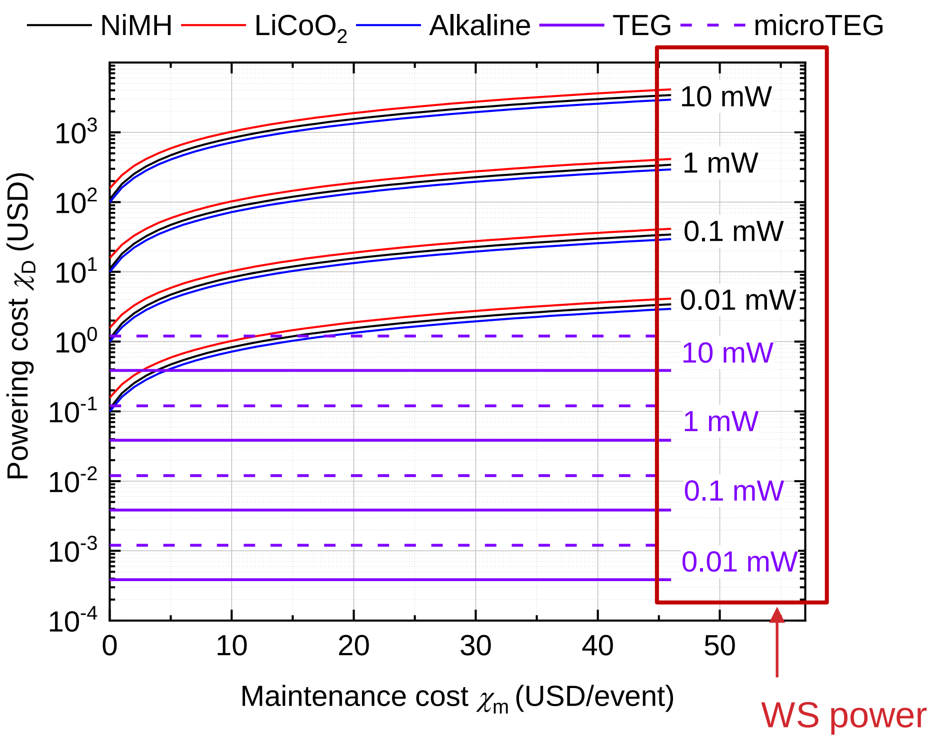

τ_D = 1,000 days

Economic metrics for batteries are USD/J (C_b) while for TEGs are USD/W (c_{TEG}). Thus, both WS lifetimes τ_D and replacement costs χ_m matter.

Note that a WSN requiring 1 mW over 1,000 days imply a battery powering cost of 9.36 USD + maintenance vs. < 0.12 USD if TEGs are used

Replacement costs depend on labor cost (5 to 23 USD/h) and duration (10 mins to 2 h): 1 to 46 USD/event.

Some Conclusions

- Research on thermoelectrics joins great fundamental challenges on materials and transport properties with applications
- Effort to develop nanomaterials has contributed to a deeper understanding of transport phenomena also at the macroscale
- Heat harvesting will remarkably contribute to the Green transition
- Low temperature micro and distributed generation are the closest area of exploitation
- Thermal management/cooling are key enabling technologies to ULSI

Credits

G.F. Cerofolini

E. Selezneva

L. Zulian

M. Arcari

S. Magagna

B. Lorenzi

E. Villa

F. Giulio

Credits

Neophytos Neophytou

Xanthippe Zianni

Ahmed Charaï
Alain Portavoce
Claude Alfonso
Marion Descoins
Domenique Mangelinck
Loïc Patout

Sandro Solmi
Matteo Ferri
Fulvio Mancarella
Francesco Moscatelli
Alberto Roncaglia
Francesco Suriano
Luca Belsito

Giampiero Ottaviani
Stefano Frabboni
Rita Tonini

Giovanni Pennelli
Elisabetta Dimaggio

FP7-NMP-2013-SMALL-7
SiNERGY Project,
Contract n. 604169

NANOthermMA Project
European Union's Horizon 2020
Grant Agreement No. 678763

Size & Aging Effect

Film characteristics after thermal processing were found to depend upon their size. Large samples systematically reported no PF enhancement.

Type	σ ($\Omega^{-1}cm^{-1}$)	α (mV/K)	PF (mW/m^2K)	Relative PF
Untreated	562	0.16	1.44	1
Small (5x50 mm^2)	544	0.55	16.5	11.4
Large (25x100 mm^2)	169	0.23	0.89	0.62
Wafers (200 mm dia.)	223	0.21	0.98	0.68

Furthermore, an additional enhancement of PFs after thermal processing in aged samples

Type	σ ($\Omega^{-1}cm^{-1}$)	α (mV/K)	PF (mW/m^2K)	Relative PF
Untreated, aged	556	0.13	1.00	0.69
Small, aged	588	0.75	33.1	23.0
Large, aged	357	0.65	15.1	10.5

The Role of Hydrogen

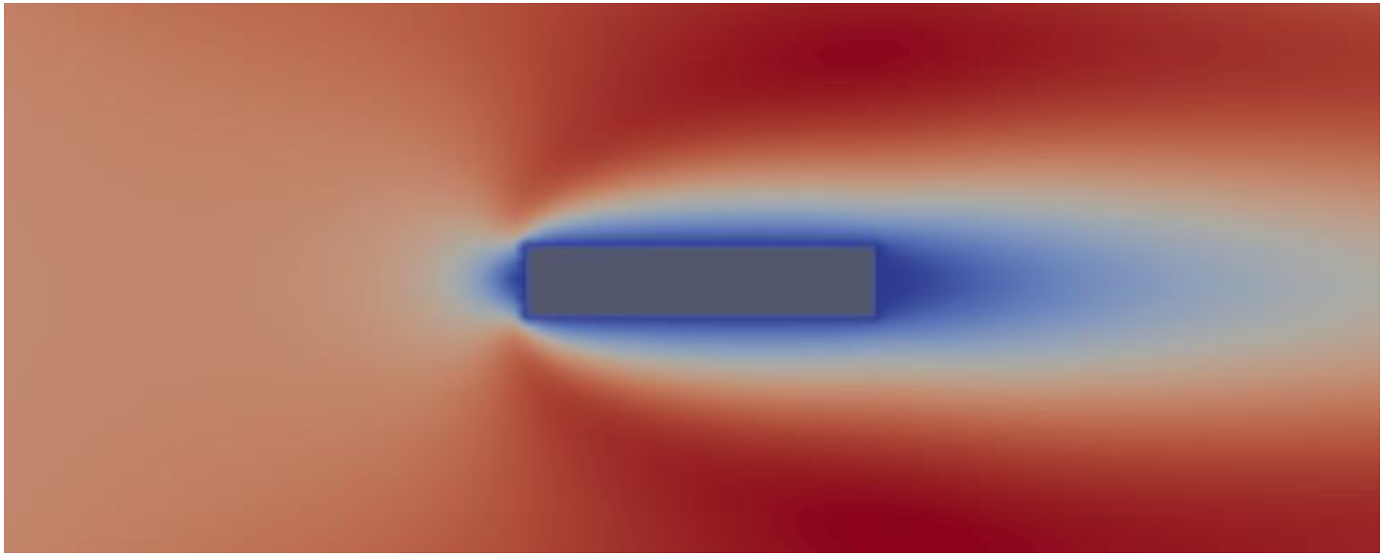

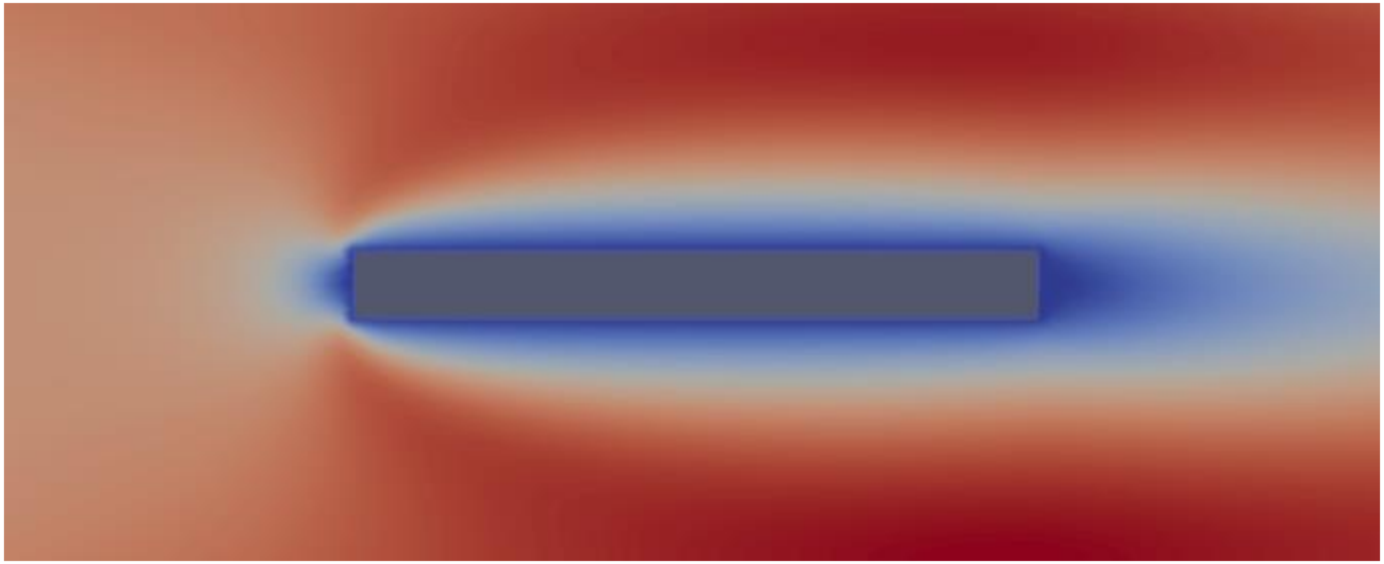

Flux: 4.26×10^{-6} m^3/s
Velocity @ 1000 °C:
1.44×10^{-2} m/s

The Role of Hydrogen

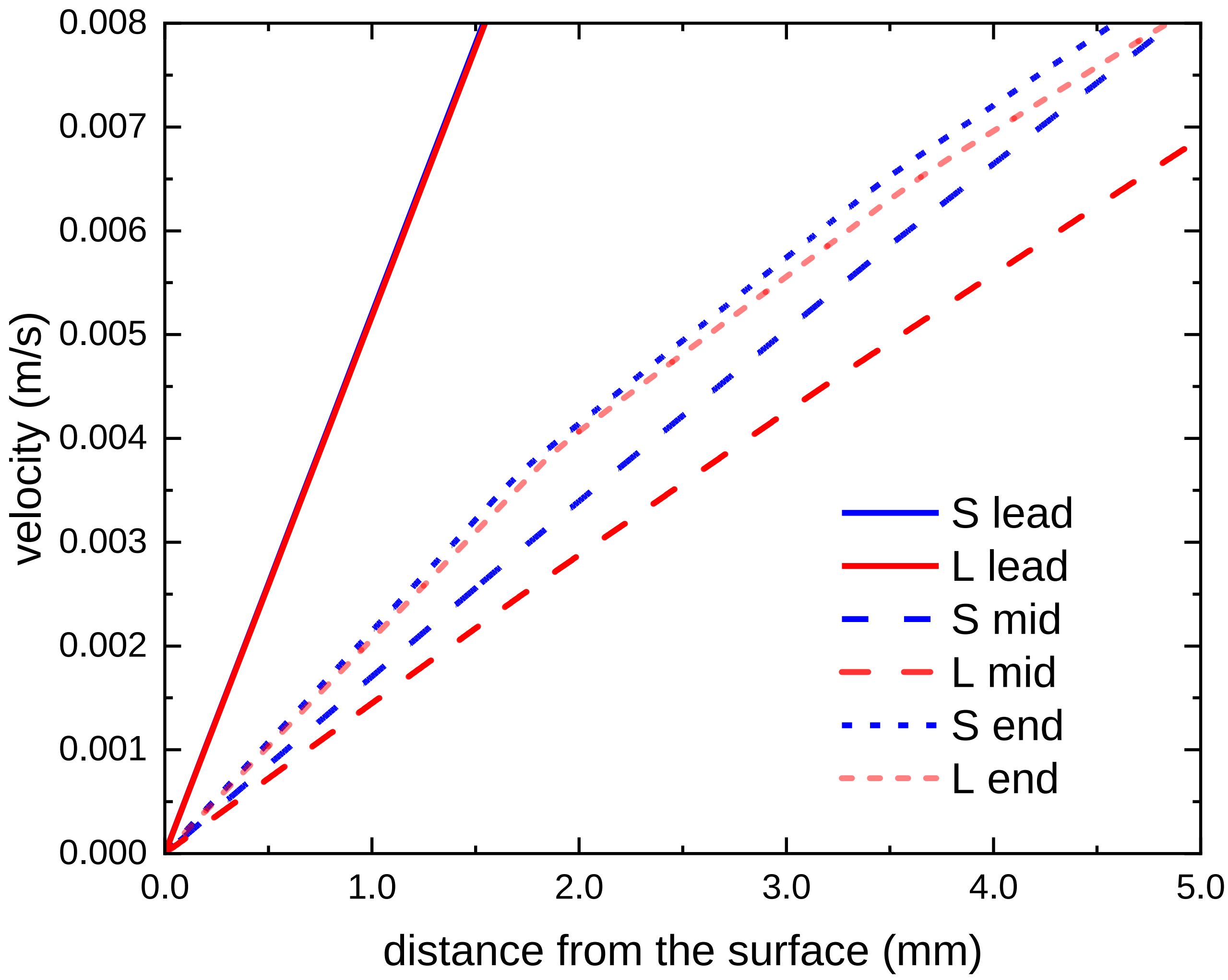

Flux: 4.26×10^{-6} m^3/s
Velocity @ 1000 °C: 1.44×10^{-2} m/s

The Role of Hydrogen

To corroborate the hypothesis, thermal processing under a tripled gas flux was performed, enabling the same velocity at film surface.

Type (tripled flux)	**σ ($\Omega^{-1}cm^{-1}$)**	**α (mV/K)**	**PF (mW/m^2K)**	**Relative PF**
Small (5x50 mm^2)	626±34	0.545±0.05	18.5±5.5	12.80±3.8
Large (25x100 mm^2)	585±31	0.63±0.06	23.4±7.0	16.25±4.9

The importance of sample size may explain why no evidence of energy filtering was reported in the past on nanosilicon thin films (grown on wafers)

D. Narducci et al., Appl. Phys. Lett., 119 (2021) 263903.

FTIR

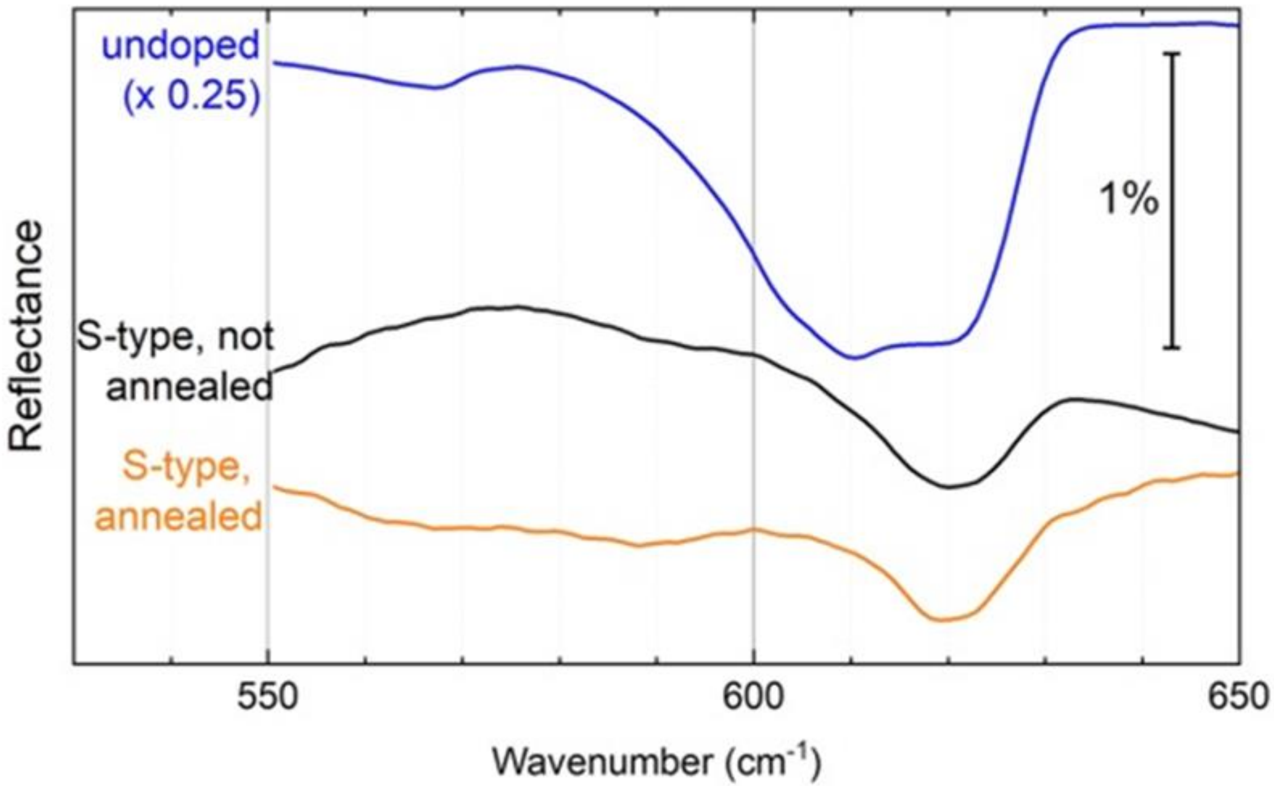
undoped
(x 0.25)
1%
S-type, not
annealed
S-type,
annealed
Reflectance
550
600
650
Wavenumber (cm-1)

Gas velocity

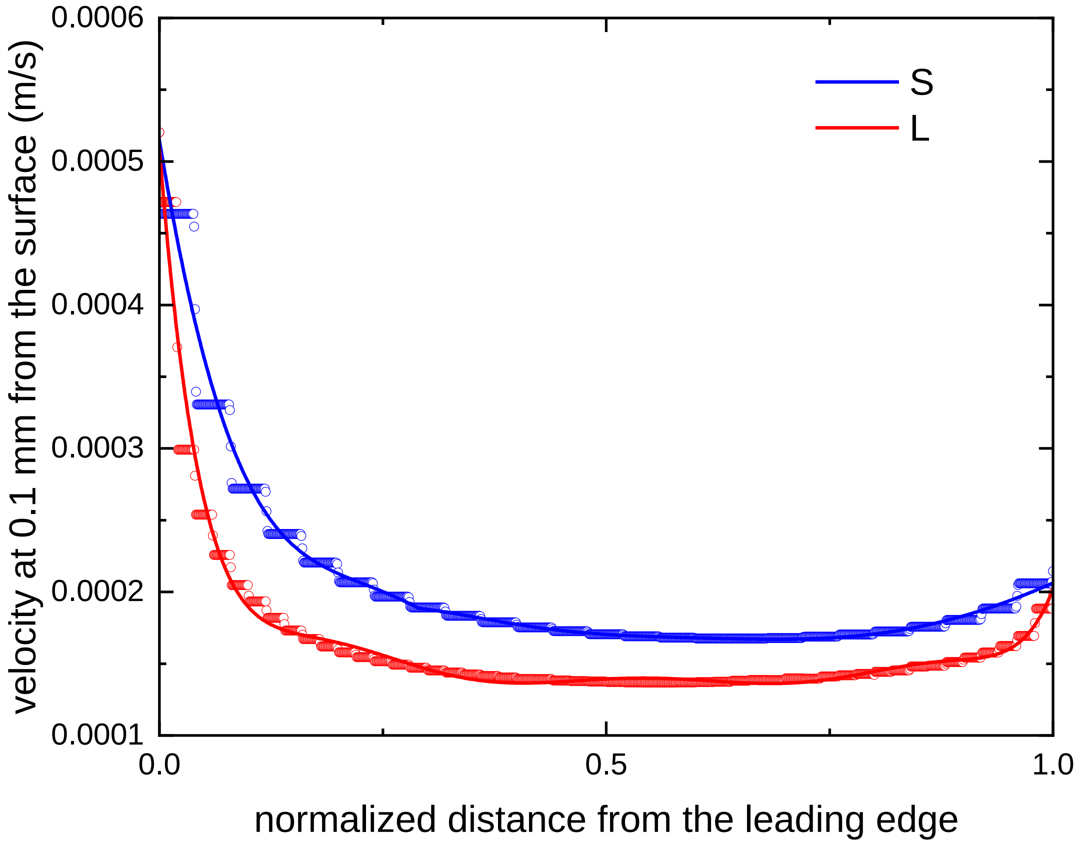

Ruling out substrate effect

- test **back-to-front current-voltage** characteristics, to test whether substrates and films are short-circuited

- switch the **substrate type**, using both n- and p-type substrates with various doping levels. No effect is observed on either Seebeck or resistivity, before or after annealing

- enhancements of the PF upon annealing at 1000 °C are **not always observed**. Systematic lack of enhancement in large samples can be hardly justified by lack of short circuits, as the size difference is by a factor 3 only

- when trying to replicate on **n-type Si thin films** (doping with P) we failed. In no case did the annealing lead to a change of Seebeck, resistivity or PF.

Silver-assisted Chemical Etching (SaCE)

Hole Exchange

Φ_{ag} = -4.72 eV

Φ_{ag} = -4.26 eV

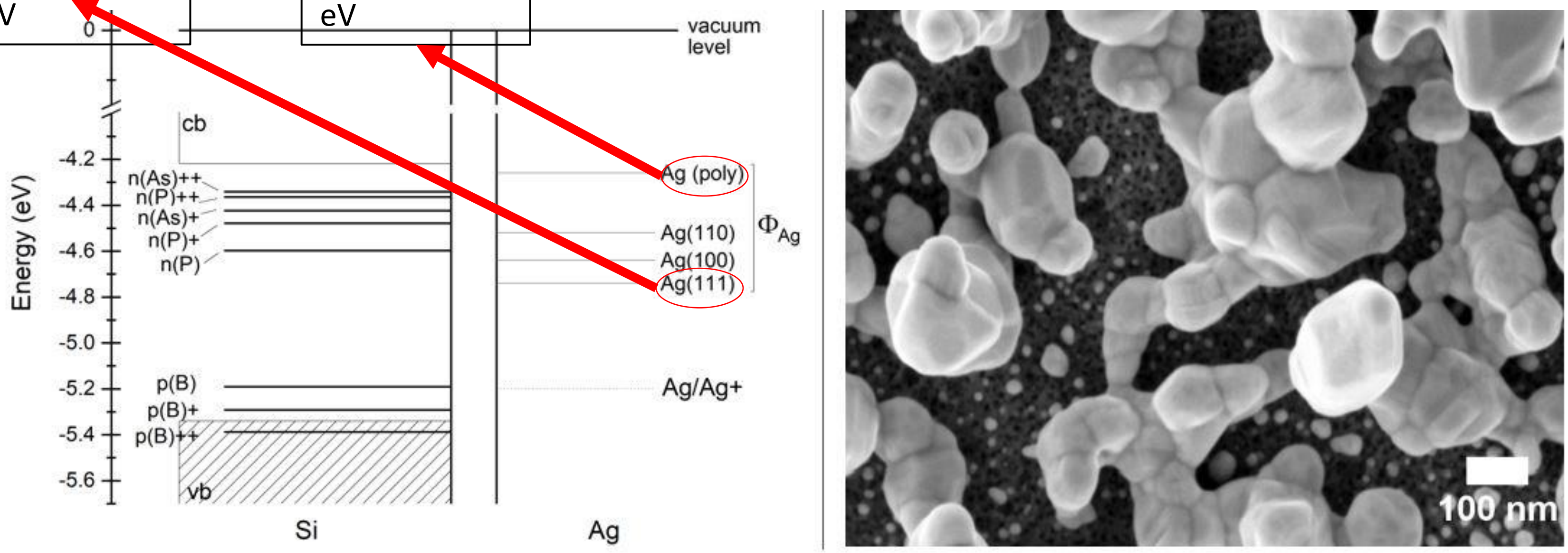

S. Magagna, D. Narducci, C. Alfonso, E. Dimaggio, G. Pennelli, A. Charaï, **Nanotechnology**, 31 (2020) 404002.

Silver-assisted Chemical Etching (SaCE)

Hole Exchange

Cathodic reaction

$Ag^+_{(aq)} \rightarrow Ag_{(s)} + h^+$

Anodic reactions

$Si_{(s)} + 4h^+ + 6H_2O_{(aq)} \rightarrow SiO_{2\,(s)} + 4H_3O^+$

$SiO_{2\,(s)} + 6HF_{(aq)} \rightarrow SiF_4{}^{2-}{}_{(aq)} + 4H_3O^+{}_{(aq)}$

4-electron process (electropolishing) Pristine Si NW formation (if localized)

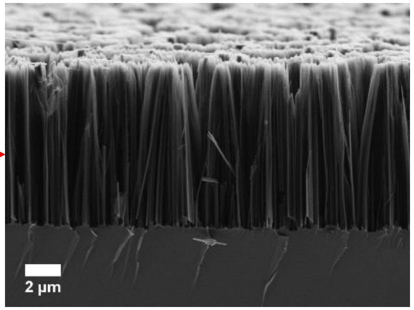

$Si_{(s)} + 2h^+ + 4HF_{(aq)} + 4H_2O_{(aq)} \rightarrow SiF_4{}^{2-}{}_{(aq)} + 4\,H_3O^+{}_{(aq)}$

$SiF_4{}^{2-}{}_{(aq)} + 2HF_{(aq)} \rightarrow SiF_6{}^{2-}{}_{(aq)} + 2H_{2(aq)}$

2-electron reaction Porous Si formation (porous NWs when localized)

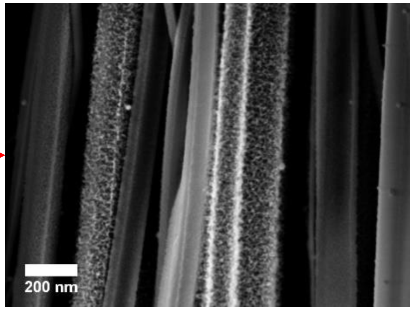

Wang et *al.,* Adv. Mater. Interfaces (**2018**), 5, 1801132

Silver-assisted Chemical Etching (SaCE)

Hole Exchange

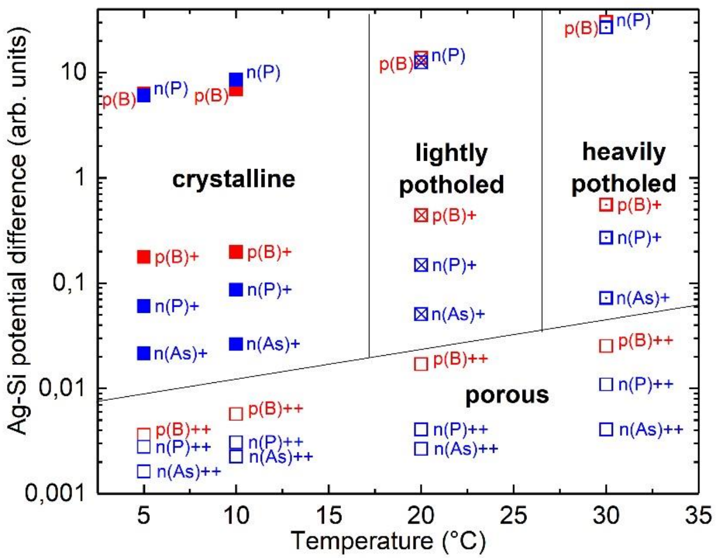

High Potential → Oxide dissolution is the **slow** reaction step →

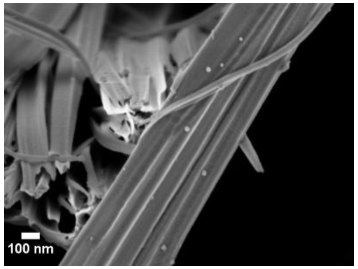

Low Potential → Oxide dissolution is the **fast** reaction step →

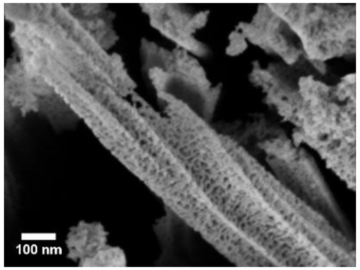

S. Magagna, D. Narducci, C. Alfonso, E. Dimaggio, G. Pennelli, A. Charaï, **Nanotechnology**, 31 (2020) 404002.

Silver-assisted Chemical Etching (SaCE)

Etching Localization

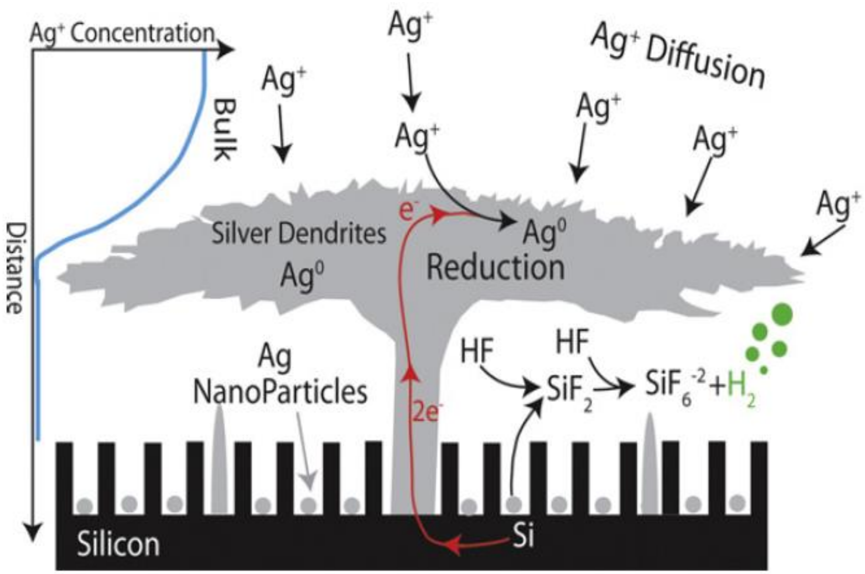

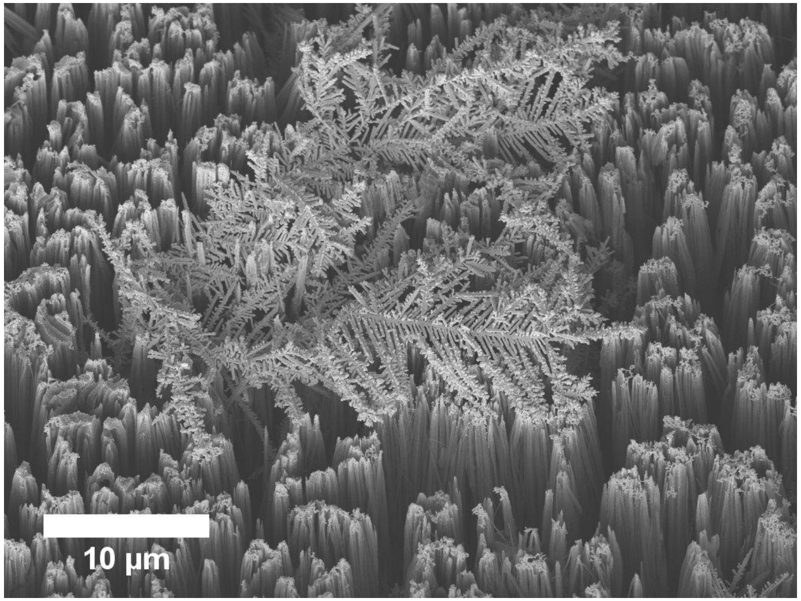

Smith et *al.,* Electrochimica Acta 92 (**2013**) 139– 147

Silver-assisted Chemical Etching (SaCE)

Etching Localization

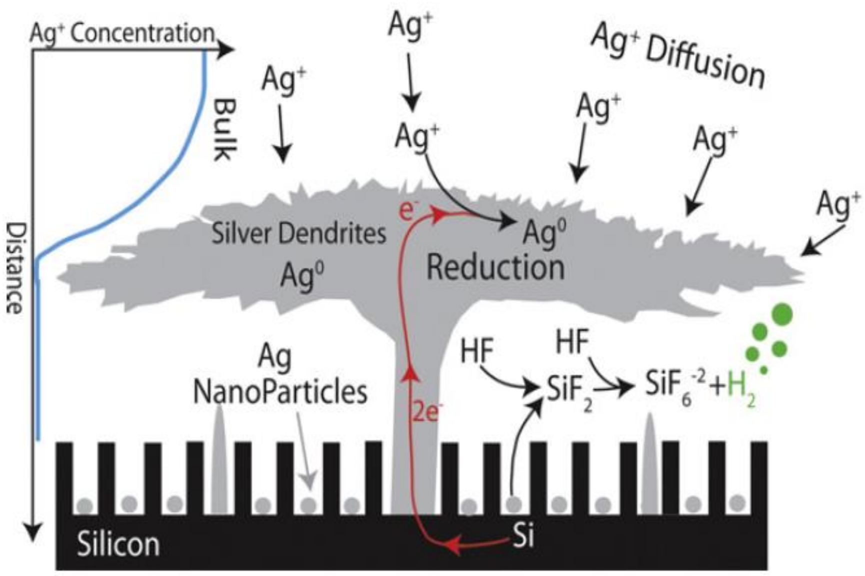

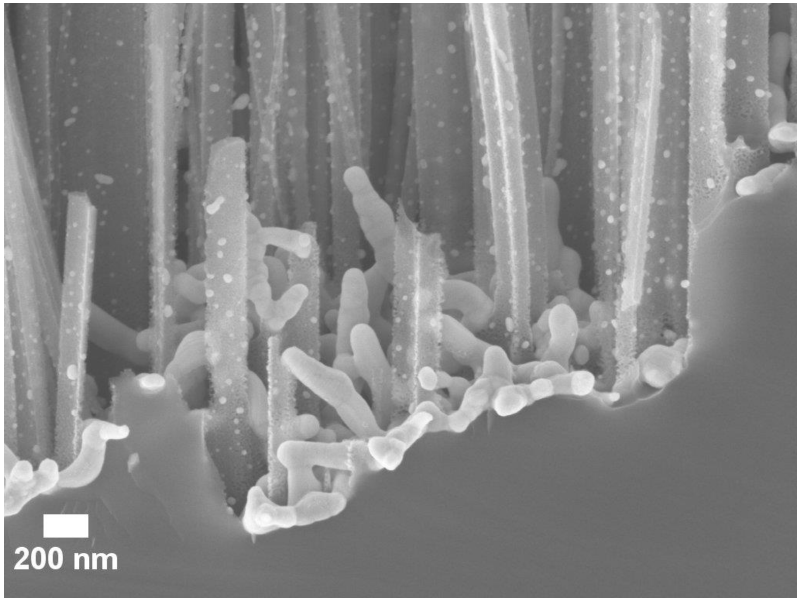

Smith et *al.,* Electrochimica Acta 92 (**2013**) 139– 147

Silver-assisted Chemical Etching (SaCE)

Etching Localization

Lateral Bores Protection

- Etching rates are identical at all {100} surfaces (on (100) silicon substrates)
- bores are overfilled by Ag dendritic structures

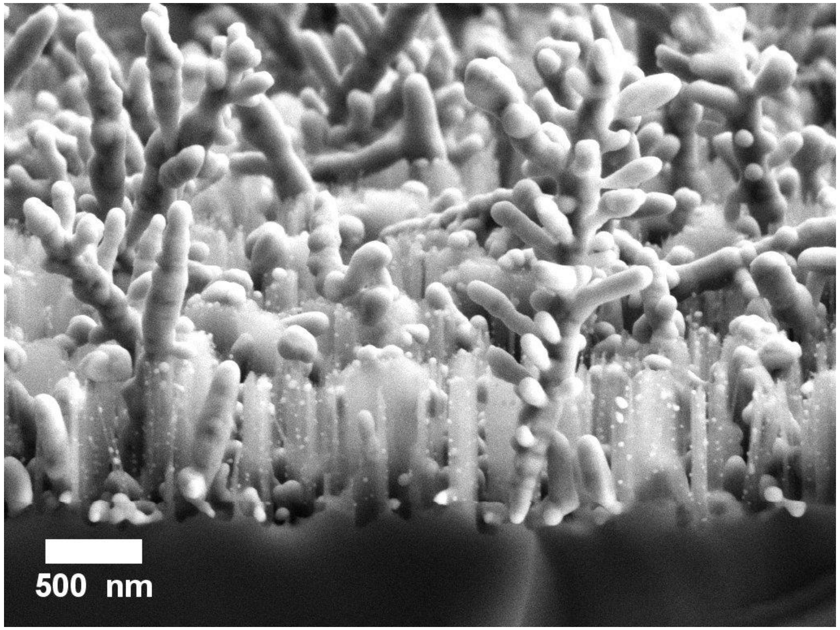

S. Magagna, D. Narducci, C. Alfonso, E. Dimaggio, G. Pennelli, A. Charaï, **Nanotechnology**, 31 (2020) 404002.

Silver-assisted Chemical Etching (SaCE)

Mechanism

10 s

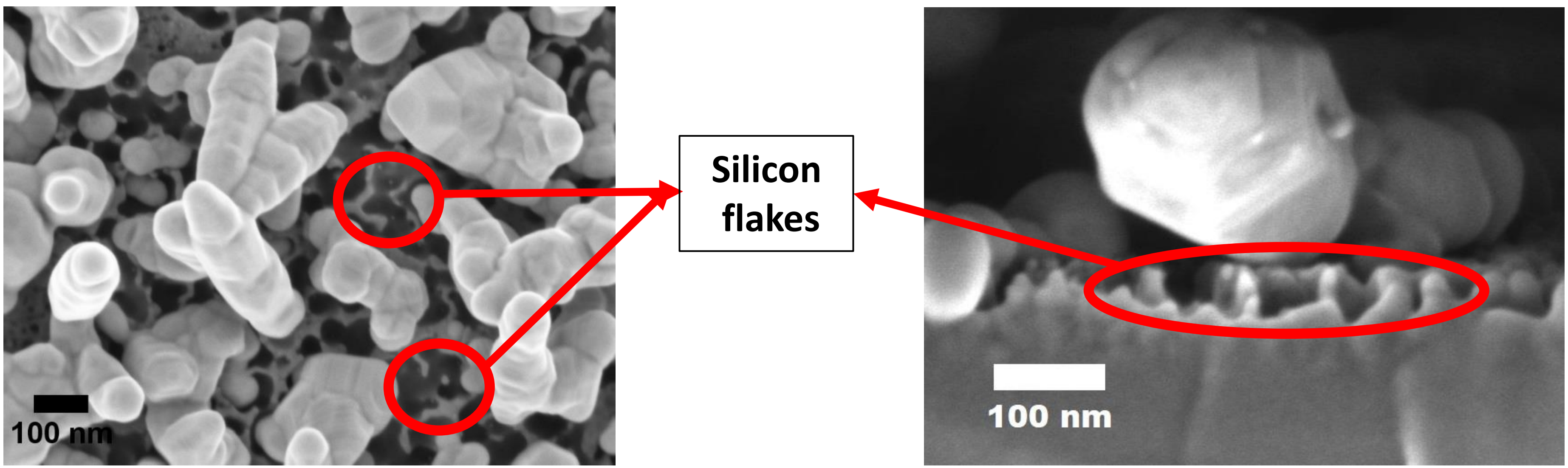

S. Magagna, D. Narducci, C. Alfonso, E. Dimaggio, G. Pennelli, A. Charaï, **Nanotechnology**, 31 (2020) 404002.

Silver-assisted Chemical Etching (SaCE)

NWs Morphology

20°C

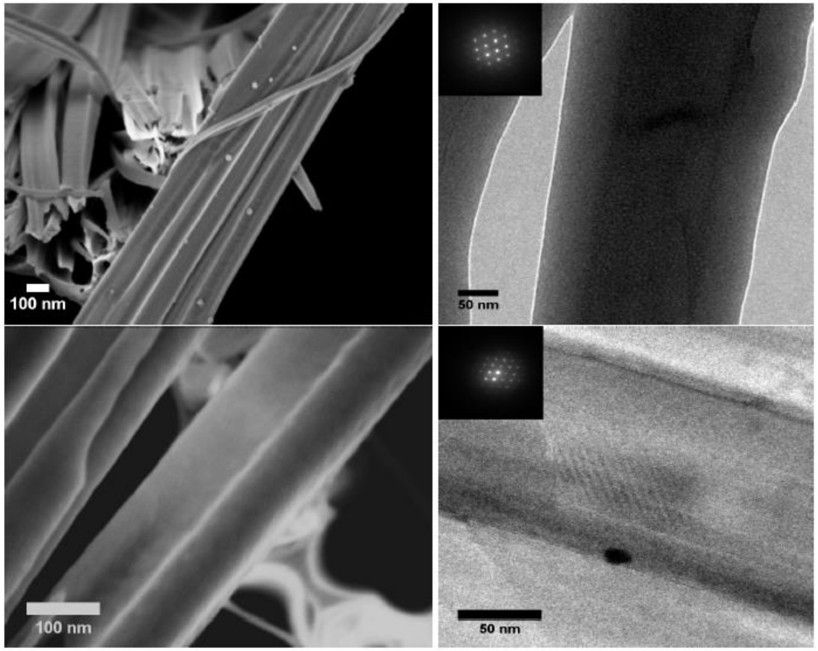

N-type (P)
Dopant Concentration~ *10*^{15} cm^{-3}

P-type (B)
Dopant Concentration~ *10*^{15} cm^{-3}

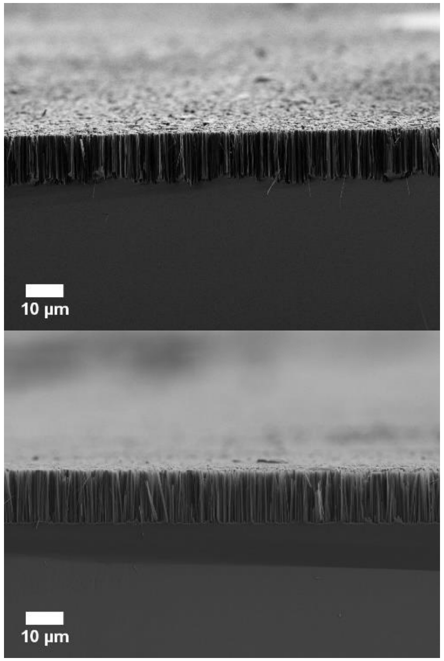

S. Magagna, D. Narducci, C. Alfonso, E. Dimaggio, G. Pennelli, A. Charaï, **Nanotechnology**, 31 (2020) 404002.

Silver-assisted Chemical Etching (SaCE)

NWs Morphology

P-type (B)
Dopant Concentration~ *10^{15}* cm^{-3}

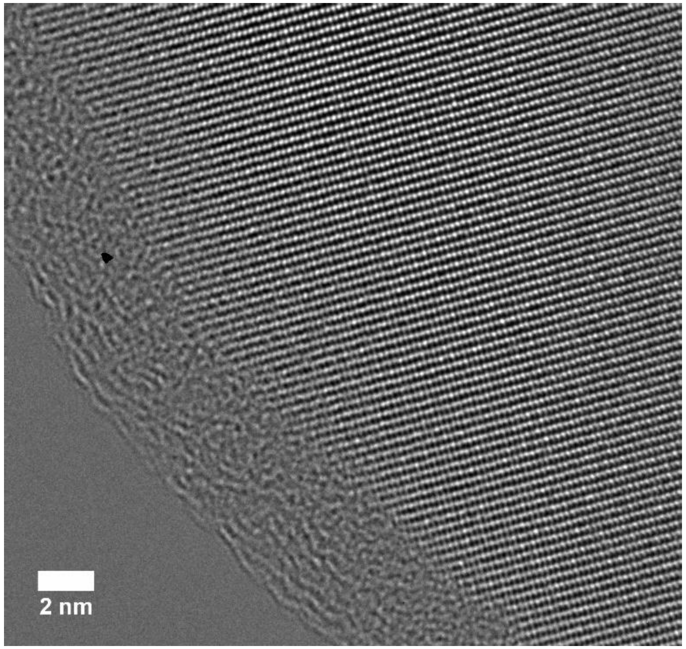

N-type (P)
Dopant Concentration~ *10^{15}* cm^{-3}

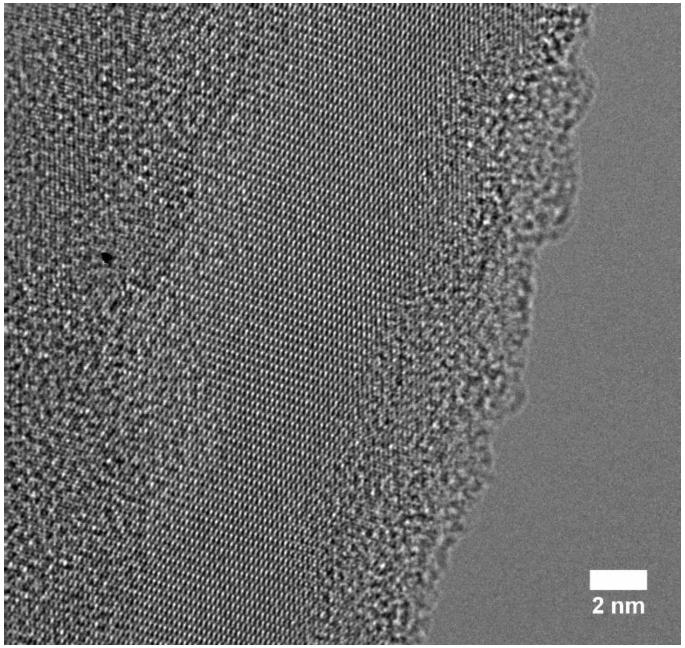

S. Magagna, D. Narducci, C. Alfonso, E. Dimaggio, G. Pennelli, A. Charaï, **Nanotechnology**, 31 (2020) 404002.

Silver-assisted Chemical Etching (SaCE)

NWs Morphology

20°C

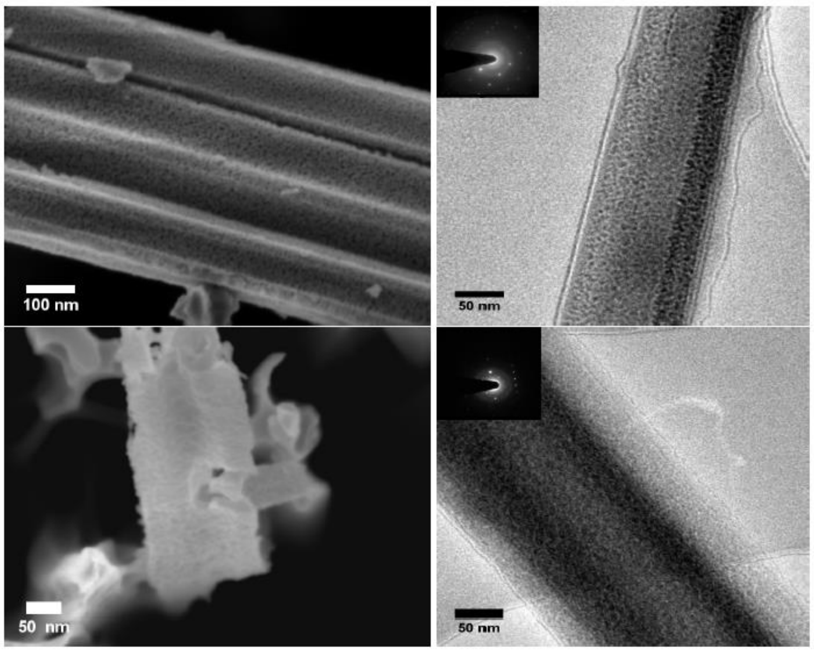

N+-type (P)
Dopant Concentration~ *10^{17}* cm^{-3}

P+-type (B)
Dopant Concentration~ *10^{17}* cm^{-3}

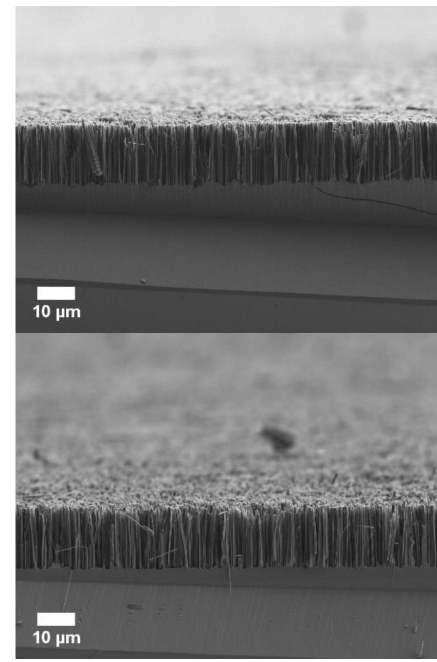

S. Magagna, D. Narducci, C. Alfonso, E. Dimaggio, G. Pennelli, A. Charaï, **Nanotechnology**, 31 (2020) 404002.

Silver-assisted Chemical Etching (SaCE)

<u>*NWs Morphology*</u>

N+-type (P)
Dopant Concentration~ *10^{17}* cm^{-3}

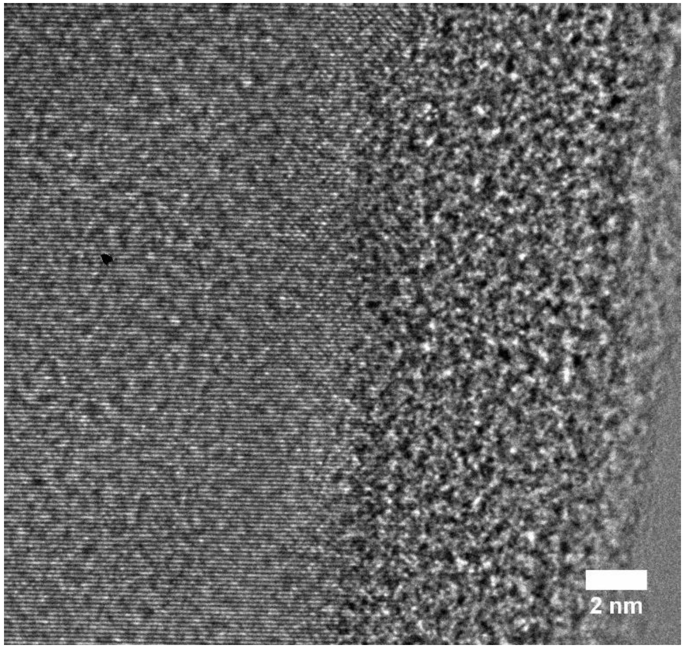

P+-type (B)
Dopant Concentration~ *10^{17}* cm^{-3}

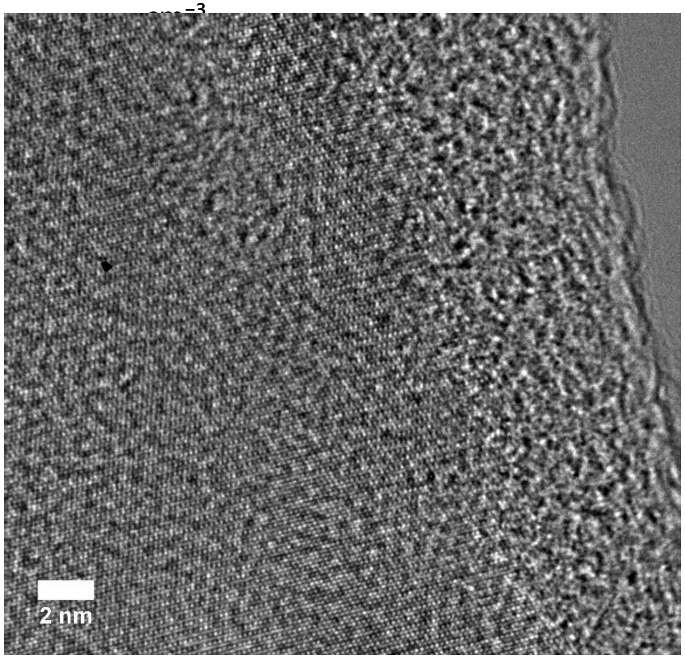

S. Magagna, D. Narducci, C. Alfonso, E. Dimaggio, G. Pennelli, A. Charaï, **Nanotechnology**, 31 (2020) 404002.

Silver-assisted Chemical Etching (SaCE)

NWs Morphology

20°C

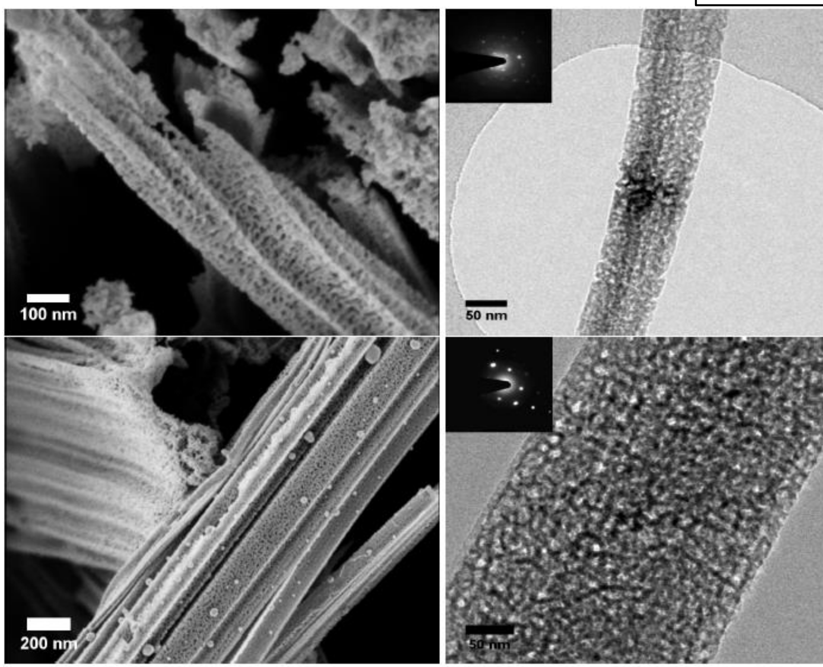

N++-type (P)
Dopant Concentration~ *10^{19}* cm^{-3}

P++-type (B)
Dopant Concentration~ *10^{19}* cm^{-3}

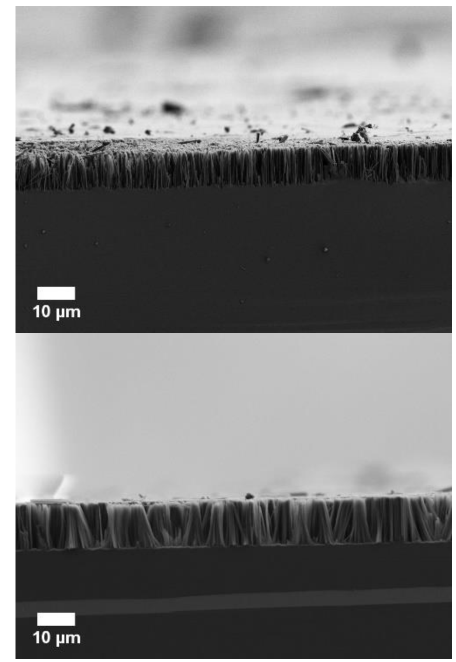

S. Magagna, D. Narducci, C. Alfonso, E. Dimaggio, G. Pennelli, A. Charaï, **Nanotechnology**, 31 (2020) 404002.

Silver-assisted Chemical Etching (SaCE)

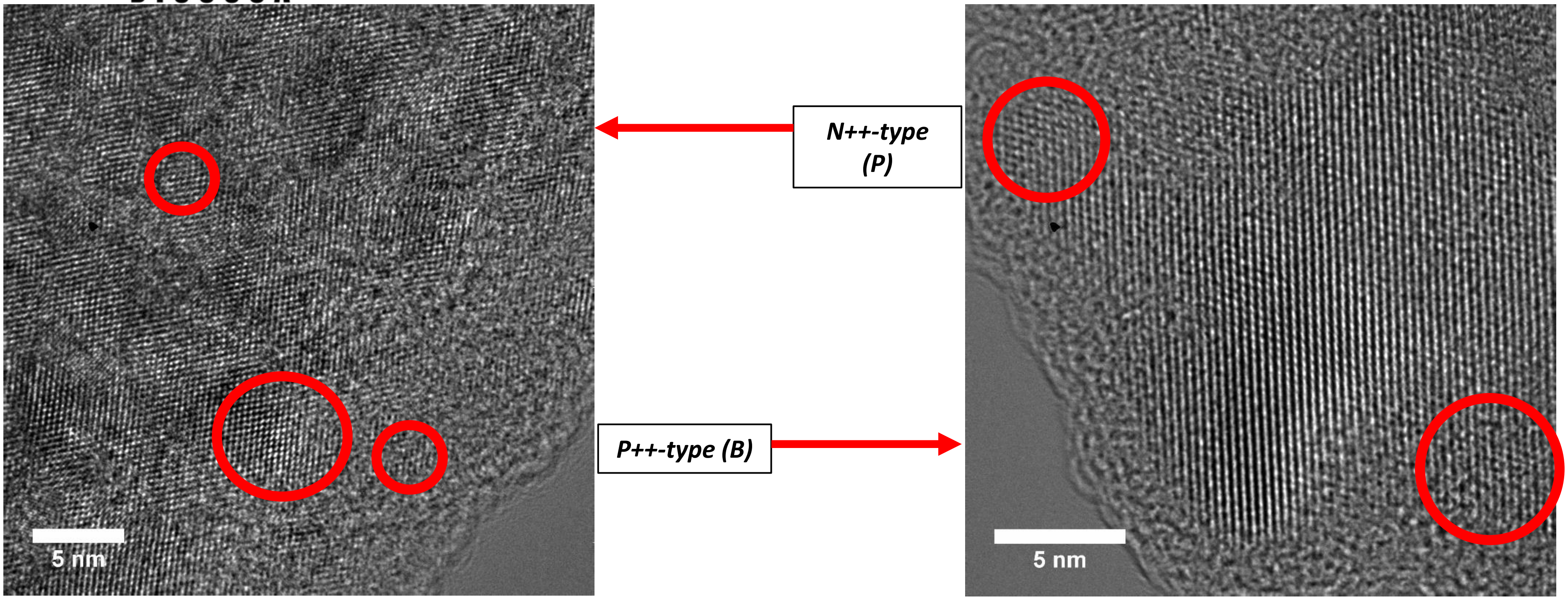

S. Magagna, D. Narducci, C. Alfonso, E. Dimaggio, G. Pennelli, A. Charaï, **Nanotechnology**, 31 (2020) 404002.